The importin-β P446L dominant-negative mutant protein loses RanGTP binding ability and blocks the formation of intact nuclear envelope

Gyula Timinszky[1,*], László Tirián[1,*], Ferenc T. Nagy[1,4], Gábor Tóth[2], András Perczel[3], Zsuzsanna Kiss-László[1], Imre Boros[4], Paul R. Clarke[5] and János Szabad[1,‡]

[1]The University of Szeged, Faculty of Medicine, Department of Biology, Somogyi B. u. 4, H-6720 Szeged, Hungary
[2]The University of Szeged, Faculty of Medicine, Department of Chemistry, Szeged, Hungary
[3]Department of Organic Chemistry, Eötvös Loránd University, Budapest, Hungary
[4]Biological Research Center of the Hungarian Academy of Sciences, Szeged, Temesvári krt. 62, H-6720, Hungary
[5]Biomedical Research Center, University of Dundee, Level 5, Ninewells Hospital and Medical School, Dundee, DD1 9SY, UK

*These authors contributed equally to this work
‡Author for correspondence (e-mail: szabad@comser.szote.u-szeged.hu)

Accepted 13 January 2002
Journal of Cell Science 115, 1675-1687 (2002) © *The Company of Biologists Ltd*

Summary

Three of the four independently induced *Ketel*^{D} dominant-negative female sterile mutations that identify the *Drosophila* importin-β gene, originated from a C4114→T transition and the concurrent replacement of Pro446 by Leu (P446L). CD spectroscopy of representative peptides with Pro or Leu in the crucial position revealed that upon the Pro→Leu exchange the P446L mutant protein loses flexibility and attains most likely an open conformation. The *P446L* mutation abolishes RanGTP binding of the P446L mutant form of importin-β protein and results in increased RanGDP binding ability. Notably, the P446L mutant importin-β does not exert its dominant-negative effect on nuclear protein import and has no effect on mitotic spindle-related functions and chromosome segregation. However, it interferes with nuclear envelope formation during mitosis-to-interphase transition, revealing a novel function of importin-β.

Key words: Importin-β, Nuclear envelope formation, Ran, Dominant-negative mutations, *Drosophila*

Introduction

About 40% of the EMS-induced dominant female sterile (*Fs*) mutations isolated in our laboratory identify genes with essential functions during the commencement of *Drosophila* embryogenesis (Erdélyi and Szabad, 1989; Szabad et al., 1989). *Ketel* is one of the *Fs*-identified genes and encodes the *Drosophila* homologue of importin-β (or karyopherin-β) (Lippai et al., 2000; Tirián et al., 2000). Importin-β is a component of the nuclear protein import machinery (reviewed by Pemberton et al., 1998; Mattaj and Englmeier, 1998; Wozniak et al., 1998; Melchior and Gerace, 1998; Weis, 1998; Görlich and Kutay, 1999). Briefly, during a 'classical' import cycle importin-β interacts with importin-α and, through importin-α, interacts with the NLS-containing nuclear protein. The three molecules form a nuclear import complex called karyopherin (Radu et al., 1995). The import complex docks on the cytoplasmic side of a nuclear pore complex (NPC). During translocation through the NPC, importin-β interacts with a number of nucleoporins, constituent proteins of the NPC. Import of the NLS-containing nuclear protein is completed on the nuclear surface of the NPC, where the import complex disassembles following the interaction of importin-β with RanGTP. Ran is a Ras-related G protein (Azuma and Dasso, 2000). While the nuclear protein stays inside the nucleus, the importin-β-RanGTP complex returns to the cytoplasm. In the cytoplasm, importin-β is released from RanGTP following the interaction of RanGTP with RanGAP (RanGTPase-activating protein) and RanBP1 (Ran-binding protein) (Bischoff and Görlich, 1997; Azuma and Dasso, 2000). Upon activity of RanGAP and RanBP1, RanGTP is converted to RanGDP, which is subsequently imported to the nucleus where it is converted to RanGTP by RCC1 (regulator of chromatin condensation), the guanine nucleotide exchange factor for Ran. The driving force of the nuclear transport process is Ran: whereas its GDP-bound form is prevalently cytoplasmic, RanGTP is generally nuclear. The different forms of Ran in the cytoplasm and nucleus are caused by the nuclear localization of RCC1 and the cytoplasmic localization of RanGAP and RanBP1 (Görlich and Kutay, 1999).

In addition to nuclear protein import, importin-β was shown to have a role in the organization of microtubules by regulating spatial and temporal distribution of microtubule-associated proteins throughout the cell cycle (Wiese et al., 2001; Nachury et al., 2001; Gruss et al., 2001). Briefly, during interphase, proteins such as NuMA and TPX2 that are required for mitotic spindle assembly are retained inside the nucleus. During mitosis, following the disassembly of the nuclear envelope (NE), the aforementioned proteins diffuse into the cytoplasm where importin-β binds and thus keeps them away from the chromatin. RanGTP was shown to be responsible for releasing proteins such as NuMA and TPX2, in the vicinity of the chromatin, from importin-β or the importin-α/β heterodimer. Ran is also involved in NE assembly by attracting and/or binding membrane vesicles (Zhang and Clarke, 2000) and is

required for vesicle fusion around chromatin (Hetzer et al., 2000).

The association of importin-β with different types of molecules during nuclear protein import cycles suggests conformational changes and, in fact, importin-β was proposed to be a rather flexible molecule (Vetter et al., 1999; Lee et al., 2000). Importin-β is composed from 19 so-called HEAT (armadillo) repeats arranged in a Spanish collar type of superhelix. It binds (1) Ran at its N-terminal region; (2) the nucleoporins with a large middle section; and (3) the importin-β binding (IBB) domain of importin-α with its C-terminal region (Kutay et al., 1997; Wozniak et al., 1998). In fact, the spatial structures of importin-β, on its own (Lee et al., 2000) and in complex with RanGTP (Vetter et al., 1999), as well as that of the IBB domain of importin-α (Cingolani et al., 1999) have recently been elucidated.

Although the *Ketel*^{D} eggs, deposited by the *Ketel*^{D}/+ females, appear normal and are fertilized, cleavage nuclei do not form inside. The *Ketel*^{D} egg cytoplasm is very toxic: when injected into wild-type cleavage embryos it hinders formation of cleavage nuclei (Tirián et al., 2000). Surprisingly, however, when injected into wild-type cleavage embryos the *Ketel*^{D} egg cytoplasm does not prevent nuclear protein import. Moreover, nuclear proteins are imported into nuclei of digitonin-permeabilized HeLa cells in the presence of ovary extracts of the *Ketel*^{D}/+ females (Lippai et al., 2000); thus revealing novel importin-β function.

In the present report we show that the replacement of Pro446 by Leu – in three of the four independently isolated *Ketel*^{D} alleles – dramatically changes the function of importin-β. We propose (based on CD spectroscopy of model peptides) that the flexibility of importin-β is reduced upon replacement of Pro446 by Leu. We show that the P446L mutant protein has no detectable affinity to RanGTP but binds RanGDP. We present evidence that the *Ketel*^{D}-encoded protein does not prevent nuclear protein import carried out by normal importin-β but inhibits NE formation at the end of mitosis. We also report that replacement of Ser317 by Thr restores characteristic importin-β functions: *Drosophila* females that lack a functional *Ketel* gene but carry a transgene with both the *S317T* and the *P446L* mutations are fully viable and fertile.

Materials and Methods

The *Ketel*^{D} alleles

The four EMS-induced *Ketel*^{D} mutations were isolated in screens for *Fs* mutations and were shown to be of dominant-negative nature (Szabad et al., 1989; Tirián et al., 2000). *Ketel*^{D1} and *Ketel*^{D3} were induced on *lt bw*-labeled isogenic chromosomes. *Ketel*^{D2} and *Ketel*^{D4} were induced on wild-type, Canton-S-derived chromosomes (Szabad et al., 1989; Erdélyi et al., 1997). The loss-of-function *ketel*^{r} alleles are recessive zygotic lethal mutations and were generated through second mutagenesis of the *Ketel*^{D} alleles (Szabad et al., 1989; Erdélyi et al., 1997). One of them, *ketel*^{rX32}, is a small deficiency that removes the *Ketel* and a few of the neighboring loci and is abbreviated as '–'. The *ketel*^{rX13} allele is transcriptionally inactive and is referred as *ketel*^{null}. The *Ketel*^{D}/– hemizygotes that perish during second larval instar were produced by crossing *y*/*y*; *ketel*^{rX32}/*y*$^{+}$*CyO* females with *y*/*Y*; *Ketel*^{D}/*y*$^{+}$*CyO* males. The *y*$^{+}$*CyO* balancer chromosome carries a *y*$^{+}$ transgene (Timmons et al., 1993). Head skeleton and the ventral setae of the *y*/*y* (or *y*/*Y*); *Ketel*^{D}/– larvae are yellow and thus allow their separation from the heterozygous nonyellow (*y*$^{+}$*CyO*) siblings in which the chitin structures are dark. [For explanation of the genetic symbols throughout the paper see (Lindsley and Zimm, 1992) and the FlyBase website http://flybase.bio.indiana.edu]. The *Drosophila* cultures were kept at 25°C.

Molecular cloning and sequencing of *Ketel*^{D1}, one of the *Ketel*^{D} alleles

DNA of *Ketel*^{D1}/– larvae served as the template in a set of PCR reactions to produce DNA fragments for sequencing. The PCR primers were designed based on the *Ketel* genomic sequence available in the EMBL nucleotide sequence database under the accession no. AJ002729. Sequencing was carried out by using the dideoxy method in an IBI automated sequenator on both strands. Results of sequencing were compared with the sequence reported for the wild-type allele (Lippai et al., 2000).

The *Ketel*^{D} (*K*^{D}) transgenes

The presumptive *Ketel*^{D1} mutation was generated through in vitro mutagenesis in PCR reactions. The generated *Bgl*II-*Cla*I fragment replaced the corresponding DNA segment in a plasmid containing a 4.0 kb *Xba-Bam*HI genomic fragment, which includes the *Ketel* promoter and the 5′ segment of the *Ketel* coding region, combined with a 2.3 kb cDNA fragment representing the rest of the transcribed part of the *Ketel* gene [see figure 1b in Lippai et al. (Lippai et al., 2000)]. The above sequences were cloned into the *CaSpeR* vector with the *mini-white* reporter gene and germ line transformants were generated by standard procedures (Thummel et al., 1988). Flies carrying the *K*^{D} transgene have orange eyes of different intensities on *white* genetic background. Three independent *K*^{D} transgenic lines were recovered. The *K*^{D} transgenes are inserted into different positions of third chromosomes and are maintained as the third chromosome-linked *Fs* mutations (Erdélyi and Szabad, 1989). The expression level of the *K*^{D} transgenes was characterized by measuring eye pigment content of *w*/*w*; *K*^{D}/+ flies. Eye pigment contents were determined by extraction of eye pigments and photometry as described by Reuter and Wolff (Reuter and Wolff, 1981). The *K*^{D} transgenes were used for the generation of +/+; *K*^{D} females and *ketel*^{null}/–; *K*^{D} zygotes.

For production of transgenes with both the *S317T* and the *P446L* mutations, we replaced a *Bgl*II-*Bst*EII fragment in the vector containing the *K*^{D} transgene with the same fragment containing the *S317T* mutation coding DNA fragment.

Production of the *Ketel*^{D}-encoded protein in bacteria

We produced normal Ketel protein as described (Lippai et al., 2000). For production of the P446L mutant protein in *E. coli*, an expression vector containing full length *Ketel* cDNA with the *P446L* mutation was generated by replacing the *Bgl*II-*Cla*I section in the pQE30 expression vector that contains the wild-type *Ketel* cDNA. Construction of the pQE30 expression vector with the wild-type *Ketel* cDNA was described previously (Lippai et al., 2000).

The expressed proteins included an N-terminal His tag that allowed purification on a nickel-NTA agarose column. Unlike the normal Ketel protein, over 95% of the *P446L* mutant protein were present in inclusion bodies. To produce functional P446L mutant protein, we dissolved the inclusion bodies in 6 M guanidine hydrochloride in the TNM buffer (50 mM Tris pH 7.5, 300 mM NaCl, 5 mM $MgCl_2$ and 5% glycerol) as used during purification of the normal Ketel protein. Renaturation of the P446L mutant Ketel protein was achieved through a 6 to 0 M decreasing guanidine gradient in TNM buffer and eluted with 0 to 0.5 M imidazole gradient in TNM buffer. The eluted protein was dialyzed against 0.1× TNM buffer overnight. Two hundred μl aliquots of the dialyzed protein were lyophilized and stored at –70°C. When used, the aliquots were dissolved in 20 μl H_2O. To test

biological activities of the purified P446L mutant Ketel protein we (1) injected it into wild-type, histone-GFP and lamin-GFP-expressing cleavage embryos; (2) used it in the nuclear import assay system with digitonin-permeabilized HeLa cells; and (3) used it in solutions to study Ketel-Ran interactions.

Injections of P446L protein into cleavage embryos

To visualize effects of the P446L molecules on cleavage embryos we carried out the following injection experiments. (1) We injected into wild-type embryos approximately 200 picolitres/egg (~2% total egg volume) from a solution that contained wild-type or P446L mutant importin-β protein (1.2 μM) and a fluorescent import substrate (0.24 μM). The fluorescent substrate was a pentamer of a fusion protein in which the nucleoplasmin core domain was combined with the importin-β-binding domain from importin-α [IBB core pentamer (Lippai et al., 2000)]. (2) The wild-type or P446L mutant importin-β solutions were injected into embryos in which the chromatin was labeled by histone-GFP protein (Clarkson and Saint, 1999). (3) The wild-type or the P446L mutant importin-β protein solutions were co-injected with a 1% solution of the 170 kDa red fluorescent TRITC (tertramethylrhodamine isothiocyanate isomer R)-dextrane. (4) Wild-type or P446L mutant importin-β was injected into cleavage embryos in which a UAS-tubulin-GFP construct (Grieder et al., 2000) was driven by a nanos-Gal4 driver. (5) The wild-type or P446L mutant importin-β solution (1.2 μM) was also injected into cleavage embryos in which a UAS-lamin-GFP construct was driven by a nanos-GAL4-VP16 driver (Van Doren et al., 1998). (The UAS-lamin-GFP transgene was kindly provided by N. Stuurman; see the FlyBase website http://flybase.bio.indiana.edu). Following injections, the fate of the injected embryos was followed through optical sections in a Zeiss LSM410 confocal microscope. The injections were done at 20°C.

The nuclear protein import assay

Digitonin-permeabilized HeLa cells were prepared by a modified protocol (Adam et al., 1990). Briefly, HeLa cells were grown on coverslips to 50-80% confluence, washed in ice-cold permeabilization buffer (20 mM Hepes-KOH pH 7.5, 110 mM potassium acetate, 5 mM magnesium acetate, 250 mM sucrose and 0.5 mM EGTA) and permeabilized for 15 minutes in the same buffer containing 60 μg/ml digitonin. The coverslips were washed three times in permeabilization buffer without digitonin. Coverslips were incubated with each 20 μl of import reaction. The import buffer contained 2 mg/ml nucleoplasmin core (to block nonspecific binding), 20 mM Hepes/KOH pH 7.5, 140 mM potassium acetate, 5 mM magnesium acetate, 250 mM sucrose, 0.5 mM EGTA. Where indicated, reactions were supplemented with an energy regenerating system (0.5 mM ATP, 0.5 mM GTP, 10 mM creatine phosphate, 50 μg/ml creatine kinase) and Ran mix [3 μM Ran-GDP, 150 nM RanGAP (Rna1p from yeast), 300 nM NTF2 and 150 nM RanBP1]. Nuclear import of the IBB core pentamer was monitored in optical sections. Import reaction samples contained 0.24 μM fluorescein-labeled IBB core pentamer, 1.2 μM wild-type or P446L mutant Ketel protein and, where indicated, Ran mix and an energy regenerating system. Reactions were stopped after 5 minutes by fixation in 3% paraformaldehyde (w/v) in PBS, washed in PBS and water, and mounted with 2 μl of vectorshield mounting medium (Vector).

Binding assays and immunoprecipitations

Binding assays were carried out as described (Hughes et al., 1998). Briefly, GST-Ran loaded with GDP or GST-RanQ69L (a RanGTP frozen form of Ran) loaded with GTP were incubated with wild-type and *Ketel^{D}* egg extracts as well as wild-type and P446L mutant Ketel proteins expressed in *E. coli* and purified as described in Lippai et al. (Lippai et al., 2000) and in this paper. Following binding Ran was pulled down by glutathione-Sepharose beads. The beads were recovered and washed, and the bound proteins were separated by SDS-PAGE and immunostained using affinity-purified anti-Ketel antibody (Lippai et al., 2000). The anti-Ketel antibody is equally efficient in recognizing the wild-type and the P446L Ketel proteins. The concentration of wild-type and P446L Ketel proteins was 0.3 μM. Protein concentrations of the egg extracts were adjusted to 18 mg/ml.

For immunoprecipitations we incubated Protein-A-agarose beads with the polyclonal anti-Ketel antibody and after thorough washing the anti-Ketel beads were given to wild-type or *Ketel^{D}* egg extracts; when indicated an energy regenerating system (0.5 mM ATP, 0.5 mM GTP, 20 mM creatine phosphate and 100 μg/ml creatine kinase) and 3 μM of wild-type or P446L Ketel proteins were added. The precipitated Ran was detected by western blot.

Enzymatic assays

Labeling of Ran with [γ-^{32}P]GTP and GTPase assays were performed essentially as described (Görlich et al., 1996). Concentration of the proteins were as follows: Ran 0.3 μM, wild-type and P446L Ketel 1 μM, RanBP1 0.4 μM, *Drosophila* RanGAP 25 nM. Hydrolysis of Ran[γ-^{32}P]GTP to RanGDP and the release of [γ-^{32}P] was measured in a liquid scintillation counter 2 minutes after bringing the components together. For measuring of nucleotide exchange activity of RCC1 on Ran, human Ran protein was loaded with [^{3}H]GTP or [^{3}H]GDP. Protein concentrations in the reactions were as follows: 0.3 μM Ran, 1 μM wild-type and P446L Ketel and 30 nM RCC1. The exchange of labeled GTP or GDP to unlabeled GDP was measured for 2, 3 and 4 minutes in a liquid scintillation counter after the components were brought together.

Structural analysis

As shown in Table 3, we synthesized two model polypeptides. (1) The first included helix B of HEAT repeat 10, the linker region plus helix A of the HEAT repeat 11 (Cingolani et al., 1999). The linker region, like the wild-type Ketel protein in the 446th position (441st in human importin-β), contained a proline (Table 3). (2) The second polypeptide differed from the first by one amino acid: the proline in the linker region was replaced by leucine.

The polypeptides were synthesized by standard solid phase technique using Boc (butyl-oxy-carbonyl) chemistry and an automated ABI 430A synthesizer (Merrifield, 1963). The crude peptides were purified by reverse-phase HPLC and characterized by mass spectrometry. The polypeptides were dissolved in (1) 100% trifluoro-ethanol (TFE); (2) a mixture of 67% TFE and 33% H_2O; and (3) 33% TFE and 67% H_2O. CD spectra of the solutions were recorded on a Jobin Yvon dichrograph Mark VI in a 0.02 cm cell. The concentration of the samples varied between 0.1-0.5 mg/ml. CD spectra were analyzed using a Convex Constrain Analysis Plus software.

Results

In three of the four *Ketel^{D}* alleles the same C4114→T transition leads to Pro446→Leu replacement

We isolated genomic DNA from *Ketel^{D1}/–* hemizygous second instar larvae and used the DNA as template in four overlapping PCR reactions. Altogether a 7869 bp segment including the promoter and the transcribed region of the *Ketel* gene was PCR amplified. The PCR fragments were cloned and sequenced. The complete sequence was subsequently compared with the wild-type nucleotide sequence of the *Ketel* gene. We noticed a C→T transition in position 4114. C4114 is part of a CC4114C code for Pro446 in the Ketel protein (Lippai et al., 2000) (see also the *Ketel* gene nucleotide sequence under accession no.

AJ002729 in the EMBL database). CTC codes for Leu and thus the $Ketel^{D1}$-associated mutant phenotype is related most likely to replacement of a single amino acid, Pro446 by Leu (P446L).

The CTC mutant sequence is part of the CTCGAG palindrome that is in fact an *Xho*I restriction site and hence the $Ketel^{D1}$-resulting C4114→T transition created a new *Xho*I restriction site. We isolated DNA from $Ketel^{D2}$/–, $Ketel^{D3}$/– and $Ketel^{D4}$/– hemizygous larvae, PCR amplified the region around the *Xho*I site and subjected the DNA to *Xho*I digestion. (As control, DNA was also isolated and *Xho*I-digested from flies that carried the founder chromosomes on which the $Ketel^{D}$ alleles were induced.) Results of *Xho*I digestion clearly revealed the presence of a new *Xho*I restriction site in the $Ketel^{D3}$ and in the $Ketel^{D4}$ but not in the $Ketel^{D2}$ allele. (Data not shown.) Apparently a common C4114→T transition is associated with three of the four independently isolated $Ketel^{D}$ mutations and all three lead to replacement of Pro446 by Leu.

The $Ketel^{D}$ (K^{D}) transgenes act as the $Ketel^{D}$ mutations

To determine whether the C4114→T transition did indeed lead to formation of three of the four $Ketel^{D}$ alleles, we generated three K^{D} transgenic lines: A, B and C, with the in vitro generated C4114→T transition inside. The K^{D} transgene became inserted into different sites on different third chromosomes. Three features of the K^{D} transgenes confirm that the $Ketel^{D}$-related phenotypes are consequences of the C4114→T transition in the *Ketel* gene.

The K^{D} transgenes completely or largely sterilize females

The +/+; K^{D} females (with two normal *Ketel* genes and one K^{D} transgene) are either sterile or their fertility is severely reduced (Table 1). Whereas the 'C' K^{D} transgenic line renders females completely sterile, as was described for the $Ketel^{D1}$/+/+ females which, in addition to $Ketel^{D1}$, carried two normal (+) *Ketel* gene copies (Tirián et al., 2000), very low offspring production rates are characteristic for lines A and B (Table 1). The variability in the female-sterilizing ability of the three K^{D} transgenic lines can be best explained by the different expression levels of the transgenes. Since the *mini-white* marker gene is also included in the K^{D} transgenes, eye pigment content of the transgenic flies is the measure of the expression level of the transgenes (Table 1). While eyes of the line 'C' flies are dark orange and reveal intensive expression of the K^{D} transgene, eyes of the line 'A' flies are light orange and reflect a low expression level. However, even the low expression level renders the +/+; line 'A' K^{D} females almost completely sterile (Table 1).

Production of offspring by the +/+; K^{D} line 'A' females provided an opportunity to recover a few +/+; K^{D}/K^{D} females. As expected, they had dark orange eyes and were completely sterile and, as in case of the $Ketel^{D1}$/+ females, embryogenesis did not commence in their eggs.

The K^{D} transgenes, like the $Ketel^{D}$ alleles, act as dominant-negative mutations

The $Ketel^{D}$ mutations are of dominant-negative type (i.e. their female sterilizing effect can be slightly reduced by extra doses of wild-type *Ketel* alleles) (Tirián et al., 2000). To determine whether the mutation in the K^{D} transgene possesses dominant-negative features, we combined the line 'A' K^{D} transgene with three different K^{+} transgene lines ('N', 'J' and 'K'; Table 2), which carry a normal *Ketel* gene inside (Lippai et al., 2000). Results of the experiment are summarized in Table 2 and clearly show the dominant-negative nature of the mutation in the K^{D} transgene: offspring production of the +/+; K^{D}; K^{+} females significantly exceeded those of the +/+; K^{D} ones ($P<0.01$; χ^2 test). The difference in the K^{D}-compensating effect of the K^{+} transgenic lines correlates well the with expression level of the *mini-white* reporter gene: the more intensively the K^{+} transgene is expressed, the more eye pigment flies have and

Table 1. Effects of the K^{D} transgenes on female fertility

	+/+; K^{D} females				
K^{D} transgene line	Tested	Offspring	Test period*	Rate of offspring production†	Eye pigment content‡
A	437	130	25.1	11.9×10^{-3}	0.169
B	76	3	7.6	5.2×10^{-3}	0.245
C	77	0	14.0	–	0.469

*Average test period per female (days).
†Offspring/(female×day). Control females with a K^{+} transgene produce ~50 offspring/(female×day).
‡Eye pigment content (OD_{485} of eye pigment solutions; see Materials and Methods).

Table 2. The combined effects of the K^{D} (line A) and the K^{+} transgenes on female fertility

		+/+; K^{D}; K^{+} females				
K^{+} transgenic line	Chromosomal location of the K^{+} transgene	Tested	Offspring	Test period*	Rate of offspring production†	Eye pigment content‡
None	–	437	130	25.1	11.9×10^{-3}	0.169
N	X	111	40	8.2	43.9×10^{-3}	0.287
J	3rd	24	10	9.3	44.6×10^{-3}	0.313
K	4th	13	8	10.2	60.2×10^{-3}	0.360

*Average test period per female (days).
†Offspring/(female×day).
‡Eye pigment content (OD_{485} of eye pigment solutions; see Materials and Methods).

the more effectively the K^+ transgene reduces K^D-imposed female sterility (Table 2).

The K^D transgenes do not support zygotic development

Efforts to construct *ketel*^{null}/–; K^D flies, that lack functional *Ketel* gene and carry one of the three K^D transgenes, failed: not a single *ketel*^{null}/–; K^D adult emerged among the well over 1000 offspring recovered in the case of each of the three K^D transgenic lines. The *ketel*^{null}/–; K^D zygotes, like the *ketel*^{null}/– and the *Ketel*^{D}/– ones die during second larval instar. Unlike the K^D transgenes the K^+ transgenes, with normal *Ketel* gene in the transgene, completely rescue lethality associated with loss of *Ketel* gene function: the *ketel*^{null}/–; K^+ flies are fully viable and fertile (Lippai et al., 2000; Tirián et al., 2000). Apparently the *P446L* mutation in the K^D transgenes behaves as the *Ketel*^{D} alleles: when paternally derived it acts as the *ketel*^{null} recessive zygotic lethal mutations.

The P446L mutant Ketel protein inhibits formation of intact NE when injected into wild-type cleavage embryos

Cytoplasm of the *Ketel*^{D} eggs is exceedingly toxic: when injected into wild-type cleavage embryos the *Ketel*^{D} egg cytoplasm prevents formation of nuclei at the end of mitosis (Tirián et al., 2000). To determine whether the P446L importin-β molecules (produced and purified from *E. coli* cells) possess the same effect as the *Ketel*^{D} egg cytoplasm, we injected small volumes of the P446L protein solution – along with a fluorescent nuclear substrate – into wild-type cleavage *Drosophila* embryos. As illustrated in Fig. 1A and D, the nuclear substrate entered the cleavage nuclei irrespectively of whether wild-type or P446L mutant importin-β protein solutions were injected. It is important to note that the P446L protein did not disrupt the NE. Similarly, ovary extracts of the *Ketel*^{D}/+ females did not block accumulation of the fluorescently labeled import substrates into digitonin permeabilized HeLa cells, and nuclei remained intact for at least 4 hours in the presence of mutant P446L protein (Lippai et al., 2000). During the upcoming mitosis the fluorescent substrate was homogeneously distributed in the egg cytoplasm around the site of injection, which indicated disassembly [that is partial in *Drosophila* (Foe et al., 1993)] of the NE and the concomitant release of the fluorescent substrate into the egg cytoplasm (Fig. 1B,E). Following termination of mitosis, in the control the fluorescent substrate entered the newly forming nuclei that doubled in number (Fig. 1C). In the P446L mutant protein, however, the fluorescent substrate remained homogeneously distributed at the site of injection (Fig. 1F). Should intact NE form, the high molecular weight fluorescent substrate would be either excluded (in the absence of nuclear protein import) from the newly forming nucleus leaving a dark outline of the nucleus, or re-imported (where nuclear protein import has resumed) in which case the nuclei would be highlighted by the fluorescent substrate, as seen in the control experiment (Fig. 1C). Since neither of the expected versions occurred, it appears that the P446L Ketel protein prevents formation of intact cleavage nuclei. Evidently, the P446L mutant importin-β exerts the same toxic effect on wild-type cleavage embryos as the *Ketel*^{D} egg cytoplasm and is very efficient in abolishing the function of wild-type importin-β molecules.

One possible explanation for the failure of cleavage nuclei formation is that the P446L molecules induced decay of the chromatin around which the NE would have assembled. To clarify the 'chromatin decay' possibility, we injected purified P446L mutant importin-β into the posterior end of cleavage embryos that expressed GFP-tagged histone highlighting the chromatin. The fate of the chromatin was followed through two rounds of cleavage divisions in the injected embryos. As time lapse recordings revealed, the P446L molecules did not hinder the upcoming chromosome segregation (Fig. 2D-F), which proceeded in almost the same way as chromosome segregation in the anterior part of the embryo that was free of P446L protein (Fig. 2A-C). While chromatin – highlighted by histone-GFP – persists at the posterior end of the embryo and forms aggregates, further cleavage cycles are accomplished at the anterior end (data not shown). Results of the histone-GFP experiments ruled out the possible decay of chromatin as the reason for the failure of cleavage nuclei formation in the presence of P446L mutant importin-β. Although chromosomes always segregated, the distance between the chromatin blocks did not grow subsequently, leading to the formation of structures that appeared as chromatin aggregates. To examine whether the formation of chromatin aggregates is the consequence of persisting or abnormally organized mitotic spindles, we injected wild-type and P446L mutant importin-β into tubulin-GFP expressing *Drosophila* cleavage embryos and monitored behavior of the mitotic spindles. As Fig. 3A-D shows, the injection of wild-type importin-β has no affect on mitotic spindle formation, shape and disassembly. Following the injection of P446L importin-β (Fig. 3E-H) mitotic

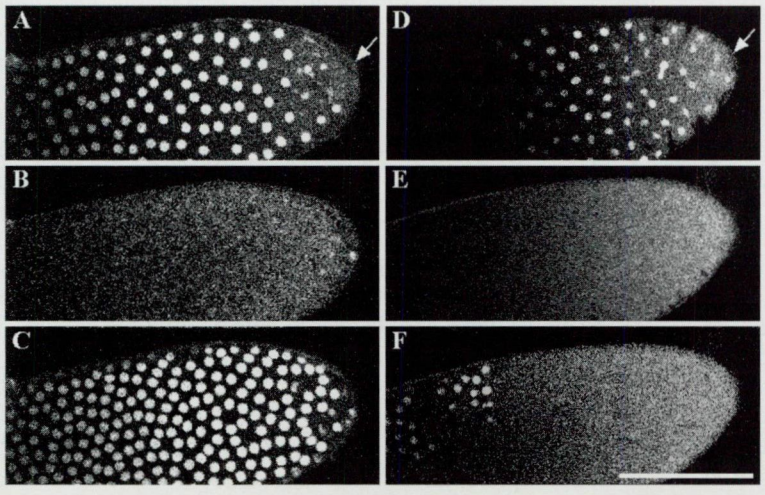

Fig. 1. Effects of the wild-type (A-C) and the P446L mutant importin-β (D-F) following their injection, along with a fluorescent nuclear substrate, into wild-type cleavage embryos. Arrows show the site of injection. Import of the fluorescent nuclear substrate into the nuclei was followed in a laser-scanning microscope. The A and D, the B and E and the C and F photographs were taken at roughly identical stages of the cleavage cycles. The few nuclei shown on F appeared following diffusion of the fluorescent substrate away from the site of injection. Bar, 100 μm.

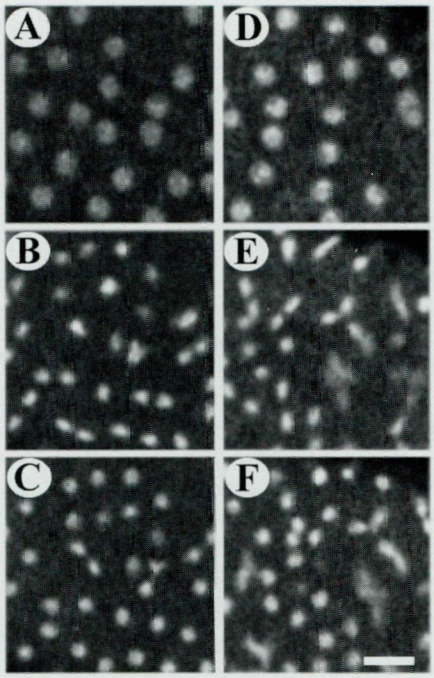

Fig. 2. Effects of P446L mutant importin-β on cleavage chromatin following its injection into wild-type cleavage embryos expressing histone-GFP. Approximately 200 picolitres P446L protein solution (1.2 μM, approximately the endogenous importin-β concentration) was injected into the posterior end of a wild-type cleavage embryo in which histone-GFP highlighted chromatin. Chromatin organization was followed in a laser-scanning microscope. Optical sections from the anterior (A-C) and the posterior (D-F) regions of the same embryo are shown. While the anterior section was devoid of P446L, the P446L mutant protein was present at the posterior region. A and D represent interphase chromatin following P446L protein injection. B and E show segregating chromosomes. C and F show chromatin during the upcoming interphase. Note that the nuclei doubled in number and the chromosomes segregate both at the anterior (control) and posterior ('experimental') regions of the embryo. Bar, 20 μm.

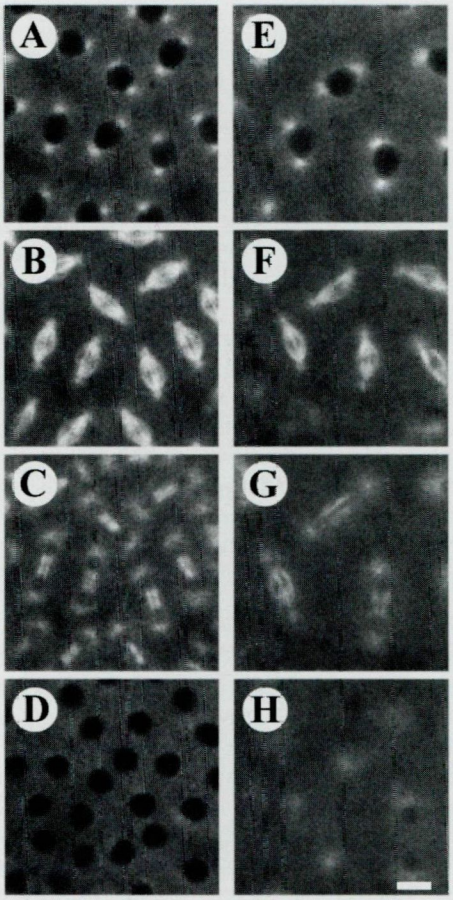

Fig. 3. Effect of P446L importin-β on cleavage mitotic spindle organization. Wild-type (A-D) or P446L mutant importin-β (E-H) solution was injected into cleavage *Drosophila* embryos expressing tubulin-GFP fusion protein. While mitotic spindle assembly, elongation and disassembly is not affected by the injected wild-type (A-C) and P446L (E-G) importin-β, the tubulin-GFP protein is homogeneously distributed in the site of P446L injection indicating the failure of NE assembly (H). Tubulin-GFP is excluded from the nuclei and appear as dark holes on the optical sections (D). Bar, 10 μm.

spindles form normally and the spindle elongation and disassembly is not affected. However, the homogenous distribution of the GFP-tubulin (Fig. 3H) indicates that NE failed to assemble since GFP-tubulin is not excluded from the space where nuclei should have formed. Failure of the chromosomes to move apart during interphase is most likely the consequence of the failure of NE formation.

To elucidate the possibility of failure of NE assembly, we conduced two further sets of injection experiments. To test whether or not intact NE forms around the chromatin in the presence of P446L protein, we co-injected a high molecular weight red-fluorescent dextrane with the P446L protein into histone-GFP expressing cleavage embryos. If intact NE is assembled around the chromatin the dextrane is expected to be excluded from the nuclei. If, however, functional NE fails to form around the chromatin, the dextrane is expected to possess an almost homogenous distribution. Following co-injection of wild-type importin-β and the red-fluorescent dextrane, the red and the green (chromatin-derived) signals were clearly separated: the green signal originated from the inside of the interphase cleavage nuclei and the red signal from the cytoplasm, which shows the formation of cleavage nuclei and hence functional NE (Fig. 4A,B). In the case of P446L and red-fluorescent dextrane co-injections the dextrane-derived signal was basically homogeneously distributed (Fig. 4D) even though the histone-GFP highlighted chromatin resembled normal interphase chromatin (compare Fig. 4A,C). Results of the above experiment are in agreement with the failure of functional NE formation in the presence of the P446L mutant importin-β.

To visualize the effect of the P446L-protein-induced NE defect, we injected wild-type (as control) or P446L mutant importin-β solutions into cleavage embryos in which lamin-GFP highlighted the lamin lining of the internal NE surface. Most of the lamin is phosphorylated upon entry into mitosis and the residual lamin-GFP molecules faintly show the so-called spindle envelope. (Cleavage mitosis in *Drosophila* is an intermediate between closed and open mitosis.) Upon entering the upcoming mitosis the lamin molecules re-enter the nucleus and highlight the NE. It is to be expected that if the P446L mutant molecules prevent NE assembly there will be no lamin-GFP signal outlining the NE at the site of injection. As Fig.

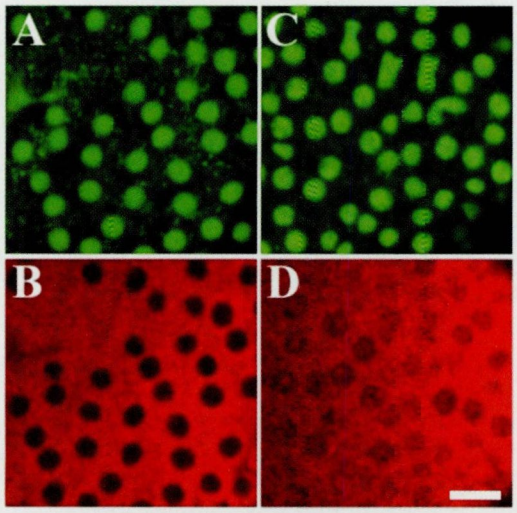

Fig. 4. Localization of the chromatin (as revealed by GFP-tagged histone; A,C) and the red-fluorescent 170 kDa TRITC-dextrane (B,D) in cleavage embryos injected with wild-type (A,B) or with P446L mutant importin-β (C,D). Following the injection of wild-type importin-β, the TRITC-dextrane is excluded from the nuclei that form following mitosis (B). However, following the injection of P446L, the TRITC-dextrane is not excluded from the region of the chromatin following mitosis (D), an indication of the absence of functional NE. Note that the chromatin morphology is hardly affected (C). Bar, 20 μm.

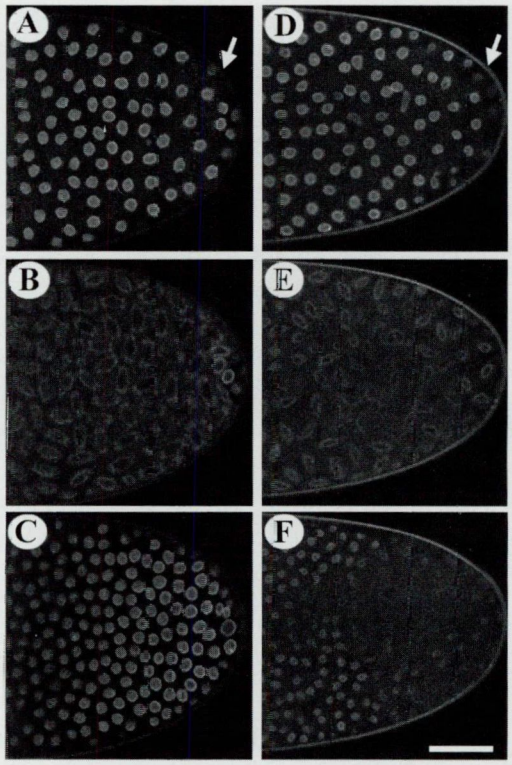

Fig. 5. Cleavage embryos expressing lamin-GFP were injected at the posterior end (arrows) with wild-type (A-C) or P446L mutant importin-β (D-F). A and D show localization of lamin-GFP during interphase following injection. The lamin-GFP molecules highlight the NE. Embryos are in metaphase in B and E, and the spindle envelopes are not affected (B,E). During the upcoming interphase, nuclear lamina re-forms in the embryos that were injected with normal importin-β (C). No nuclear lamina assembles at the site of injection of the P446L mutant importin-β revealing the failure of intact NE formation (F). Bar, 50 μm.

5A-C shows, following the injection of wild-type importin-β the lamin-GFP molecules highlight the NE during the upcoming interphase. Upon entry to mitosis, most lamin molecules diffuse into the cytoplasm and only some remain attached to the spindle envelope (Paddy et al., 1996) (Fig. 5B). Following chromosome segregation the NE reassemble as pictured by formation of the green fluorescent lamin lining (Fig. 5C). When the P446L mutant protein is injected into the lamin-GFP-expressing cleavage embryos, the lamin disappears during mitosis as in the control experiment showing that mitosis is not affected until late anaphase (Fig. 5D-F). In the presence of the P446L molecules, however, the lamin lining never re-forms, which shows the failure of intact NE assembly.

The above injection experiments show that the P446L importin-β molecules interfere with the formation of intact cleavage nuclei and the defect is manifested during the mitosis-to-interphase transition through the prevention of intact NE assembly. The *Ketel*^{D} mutations possess dominant-negative action on NE assembly and impede function of the normal importin-β molecules and thus reveal a novel role of importin-β required during NE formation at the end of mitosis. The novel importin-β function is distinct from both its role in nuclear protein import and the recently described function in mitotic spindle assembly (Wiese et al., 2001; Nachury et al., 2001; Gruss et al., 2001).

The P446L mutant importin-β allows formation and docking on the NE of the import complexes but does not support nuclear protein import

As described earlier, the wild-type importin-β molecules support import of NLS-containing substrates into nuclei of digitonin-permeabilized HeLa cells (Lippai et al., 2000). Interestingly, ovary extracts of the *Ketel*^{D}/+ females, with both wild-type and P446L mutant protein inside, support nuclear protein import as efficiently as ovary extracts of wild-type (+/+) females (Lippai et al., 2000). As presented above, when injected into wild-type embryos the P446L mutant protein does not prevent import of a nuclear substrate into the cleavage nuclei. Two feasible possibilities seem to account for the above phenomena: (1) it may be that, although the P446L mutant protein molecules do not participate in nuclear protein import, they do not prevent function of the wild-type importin-β molecules to accomplish their function; or (2) perhaps P446L mutant importin-β supports nuclear protein import. To determine which of these two possibilities is true we analyzed behavior of the P446L mutant protein in the nuclear protein import assay. As illustrated in Fig. 6, in the presence of only the fluorescent nuclear substrate and importin-β or the P446L mutant protein, although in reduced amounts, nuclear import complexes form and dock on the cytoplasmic surface of digitonin-permeabilized HeLa cell nuclei (Fig. 6A,C). The higher cytoplasmic background, in the case of P446L, is most likely the consequence of the altered structure of the P446L molecules (see below) leading to association of the import

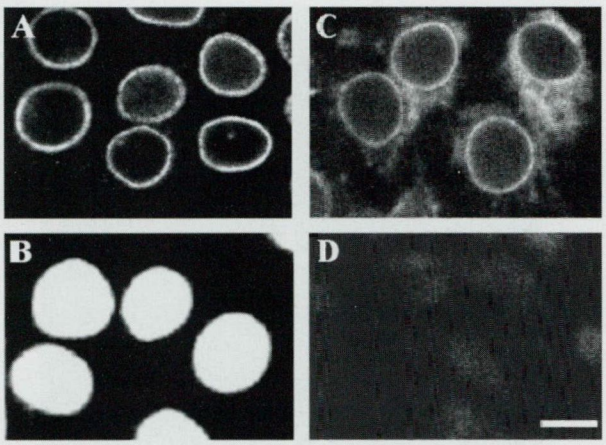

Fig. 6. Nuclear import complexes form and dock on the NE of the digitonin-permeabilized HeLa cells following the addition of either wild-type (A) or P446L mutant importin-β (C) in the presence of the fluorescent IBB-nucleoplasmin fusion protein. Upon addition of the import mixture (the fluorescent IBB-nucleoplasmin fusion protein, Ran, NTF2, RanGAP, RanBP1 and energy supply) and the wild-type importin-β, nuclear import complexes form and enter the nuclei (B). However, when P446L mutant importin-β is added along with the import mixture, import complexes do not form and the HeLa cell nuclei are not highlighted by fluorescent signal (D). Bar, 10 μm.

cargo/P446L importin-β with cytoplasmic structures, possibly membranes or microtubules. In the presence of normal importin-β and when further components of nuclear import are added (i.e. Ran, NTF2, RanGAP, RanBP1 and energy supply) the complexes are imported into the nuclei (Fig. 6B). In the case of the P446L mutant protein, however, import complexes do not form (Fig. 6D) as revealed by the absence of fluorescent signal in the HeLa cells.

Results of the above experiments show that the P446L mutant protein does not support nuclear protein import. However, as the above-mentioned injection experiments and nuclear import assays with ovary extracts of *Ketel*^{D}/+ females revealed (Lippai et al., 2000; Tirián et al., 2000), they do not hinder nuclear import accomplished by the normal importin-β molecules. Apparently effects of the P446L mutant protein are manifested only during the mitosis-to-interphase transition in preventing intact NE formation.

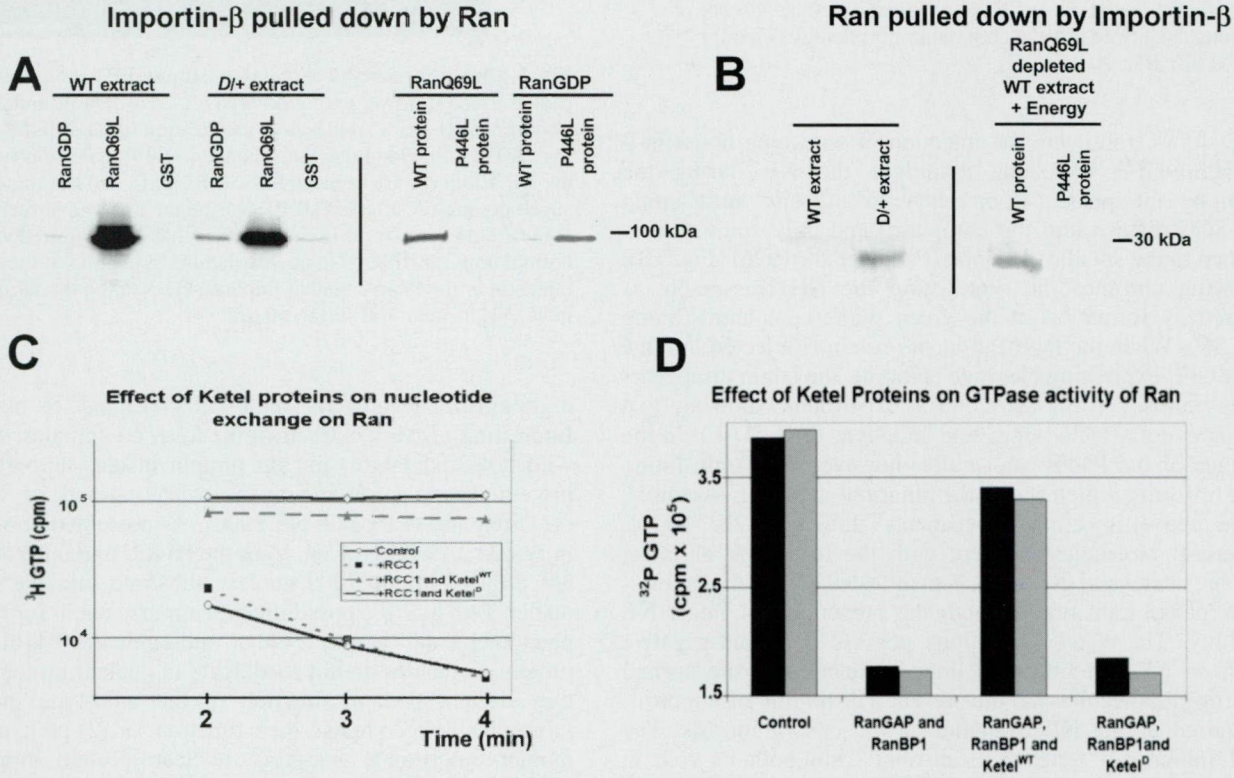

Fig. 7. RanGDP removes higher amounts of importin-β from extracts of *Ketel*^{D} eggs than from extracts of wild-type (WT) eggs. RanQ69L protein binds higher amounts of importin-β protein from WT egg extract than from extract of *Ketel*^{D} eggs. GST protein was used as a negative control (A, left). RanQ69L protein removes high amounts of purified WT importin-β but not purified P446L mutant protein. At the same time RanGDP removes higher amounts of purified P446L importin-β compared with the purified WT importin-β (A, right). More Ran is precipitated with the anti-Ketel antibody from extracts of the *Ketel*^{D} eggs than from extracts of WT eggs. (B, left). However, if an energy-regenerating system and 3 μM (10 times the endogenous importin-β concentration in the extract) purified wild-type or P446L mutant importin-β are added to WT egg extract, more Ran is precipitated from the extract supplemented with WT importin-β (B, right). Wild-type importin-β inhibits both exchange of the labeled GTP from Ran (C) and GTP hydrolysis (D), whereas P446L mutant importin-β has no effect on both nucleotide exchange and GTP hydrolysis. In C, the time course of nucleotide exchange is shown on a semi-logarithmic scale and D shows the results of the reactions performed in duplicate.

The *P446L* mutant protein loses affinity to RanGTP but binds RanGDP

Changes in the Ran-binding ability of the P446L protein are suggested by the fact that the P446L molecules are unable to accomplish nuclear protein import in the digitonin-permeabilized HeLa cells (Fig. 6D). To examine this possibility, we tested the binding of wild-type and P446L importin-β to different GST-Ran fusion proteins in solution binding assays (Fig. 7A). Apparently, RanGDP binds significantly higher amounts of importin-β from *Ketel*^{D} egg extracts than that from wild-type *Drosophila* egg extracts. Since Ran is mainly in its GDP-bound form in cytoplasmic extracts, the above result suggests increased RanGDP binding affinity of the P446L protein. Conversely, RanQ69L loaded with GTP binds higher amounts of importin-β from wild-type egg extracts than that from *Ketel*^{D} extracts, suggesting reduced binding ability of P446L to RanGTP. As a negative control we used GST protein alone, which showed only background binding levels with both P446L and wild-type importin-β. Since the *Ketel*^{D} egg extracts contain 50% wild-type importin-β, the extracts are not suitable to examine the RanGTP binding ability of the P446L protein. To confirm the reduced affinity of P446L to RanGTP, we measured the amount of the pulled down importin-β proteins from solutions containing purified wild-type or P446L mutant importin-β. As shown in Fig. 7A, wild-type importin-β binds strongly to RanQ69L, but the P446L protein shows only background binding to RanQ69L. (RanQ69L is a GTP-loaded GTPase deficient mutant Ran protein.)

To support the altered binding of P446L to Ran, we carried out immunoprecipitations with the polyclonal anti-Ketel antibody. The amount of precipitated endogenous Ran was higher from *Ketel*^{D} egg extracts compared with wild-type egg extracts. However, if an energy regenerating system and purified wild-type or P446L importin-β is added to the wild-type extract, more Ran is precipitated from the extract supplemented with the wild-type importin-β (Fig. 7B). The shift in Ran binding ability following addition of an energy supply correlates with the ability of wild-type importin-β to bind RanGTP and the inability of P446L to do so. Results of the described experiments are further supported by the enzyme assays described below.

Importin-β has been known to inhibit both GTP hydrolysis on Ran and the exchange of RanGTP catalyzed by RCC1. We studied, in solutions, the effects of the purified importin-β and P446L proteins on both nucleotide exchange and GTP hydrolysis on Ran. The wild-type Ketel protein inhibits both GTP nucleotide exchange and GTP hydrolysis, whereas the *Ketel*^{D} encoded protein has no effect on the processes (Fig. 7C,D), which shows that the P446L mutant protein cannot bind to RanGTP. Neither wild-type nor P446L have significant effect on nucleotide exchange from RanGDP (data not shown). In conclusion, the failure of functional NE formation may be the consequence of the altered RanGTP binding ability of the P446L mutant importin-β.

The *P446L* mutation appears to increase helix content and reduce flexibility of the encoded protein

As described above, the C4114→T transition leads to replacement of a helix-breaking Pro by Leu in position 446. It may be that in the P446L mutant protein the Pro446→Leu exchange leads to fusion of two adjacent helices, namely the B helix of HEAT repeat 10 and the short helix in the linker region towards helix A of HEAT repeat 11. To test whether helix content of the P446L molecules is indeed increased compared with the wild-type importin-β molecules, we synthesized two model peptides representing the noteworthy region in importin-β. We then carried out CD spectroscopy of the peptides that were dissolved in the apolar solvent trifluoro-ethanol (TFE) or in mixtures of TFE and water (Fig. 8). CD spectroscopy has been known to be a sensitive technique to analyze protein structures: CD spectra recorded in different polarity molecular environments (i.e. in solvents with different dielectric constant) often reveals structural changes (Perczel et al., 1991; Perczel et al., 1992).

In 100% TFE, which provides low polarity and a membrane mimicking environment, both model peptides resulted in so-called C-type CD spectra, which refers to a mixture of β-turns (type I or III) and α- (or 3_{10}) helices (Perczel et al., 1991). Ordered structure of the peptides is revealed by (1) the presence of the two shoulders in the spectra at 209 and 224 nm (the ππ* and nπ* transitions, respectively) and also by (2) reaching the 209 nm shoulder lower Θ values as the 224 nm shoulder (Fig. 8). CD spectra of the Pro-containing peptide – representative of the wild-type importin-β – reveal high α-helix content in both TFE and mixtures of TFE and water and the spectra changed significantly along with increase in water content of the molecular environment, reflecting flexibility of the peptide (Fig. 8A). Results of CD spectroscopy are in line with the previously published 3D structure of the aforementioned segment of importin-β (Cingolani et al., 1999; Lee et al., 2000) and are illustrated in Fig. 9B: amino acids that comprise HEAT repeats in 10B and 11A form α-helices and are interconnected with a β-turn. There is a short, three amino acid α-helix starting with Pro446 in the turn region adjacent to HEAT repeat 10B.

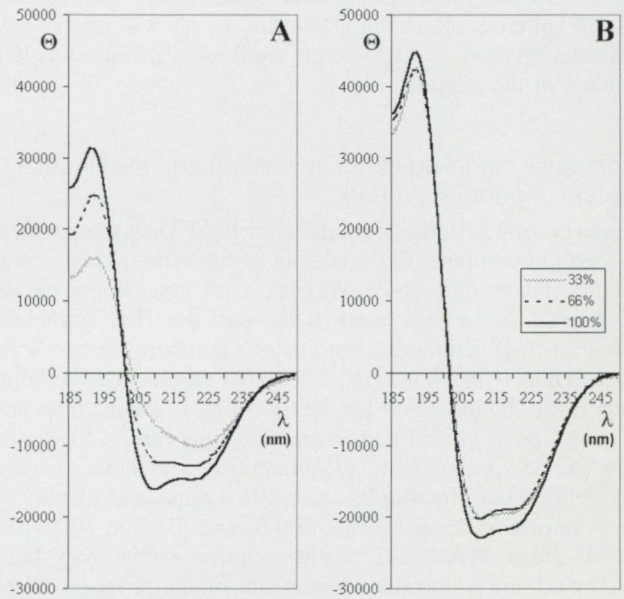

Fig. 8. CD spectra of model peptides representing wild-type (A) and P446L mutant importin-β (B). The CD spectra were recorded in 100% trifluoro-ethanol (TFE, continuous lines), in a mixture of 66% TFE and 33% H_2O (dashed lines), and in 33% TFE and 66% H_2O (dotted lines).

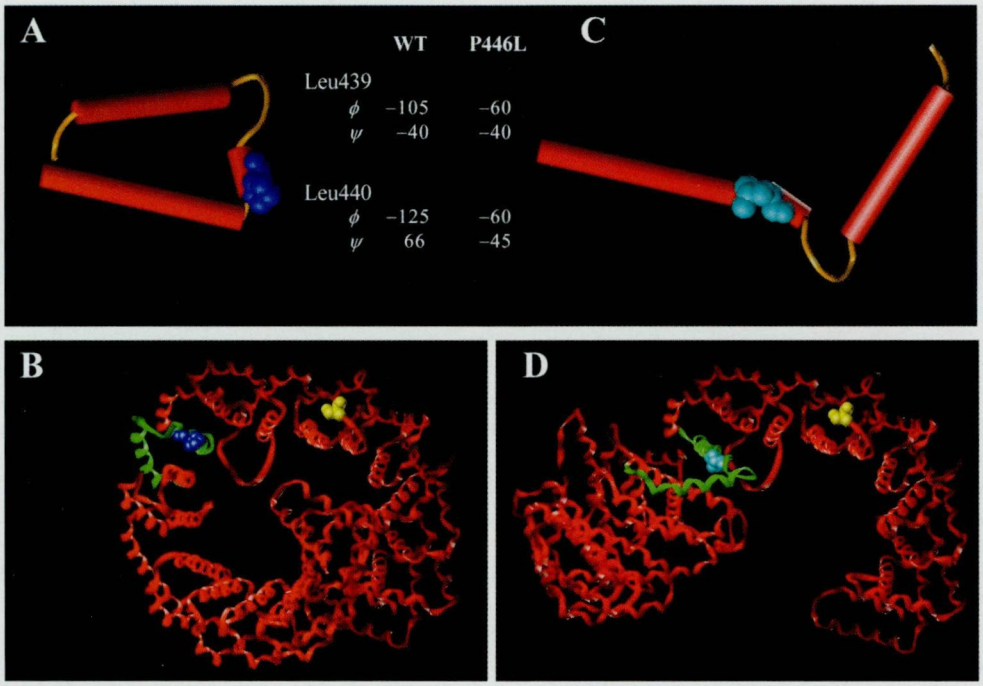

Fig. 9. Computer modeling of the structure of model peptides (A,C) and importin-β (B,D) with Pro (A,B) and Leu (C,D) in the linker region between HEAT repeats 10 and 11. In computing the structure of the peptides and the proteins only three angles were changed as shown on the figure. Leu439 and Leu440 are Ile444 and Ile445 in *Drosophila*. Pro, Leu and Ser in the critical position appear dark blue, light blue and yellow, respectively.

In contrast to the Pro-containing peptide, CD spectra of the Leu-containing model peptide, representing the P446L mutant protein, remained essentially unchanged on increasing the water content (i.e. the dielectric value) of the medium, which shows that the Leu-containing peptide, while keeping its predominantly helical organization, loses flexibility compared with the Pro-containing peptide (Fig. 8B). It appears that in the presence of water, helices of the Pro-containing peptide undergo a limited untwisting and/or rearrangement of the helix-turn-helix conformation and the Pro→Leu exchange results in a mutant molecule that lost flexibility. An illustration of the altered molecular structure is shown in Fig. 9D, considering that the Pro→Leu exchange increased α-helix content of the peptide.

Computer modeling of the importin-β and the P446L mutant importin-β proteins

Based on results of the formerly described CD spectroscopy, we carried out computer 3D modeling of both the normal and the P446L mutant importin-βs. We took X-ray crystallographic data of human importin-β associated with the IBB domain of importin-α. [For atomic coordinates of importin-β see access code 1QGK (Cingolani et al., 1999).] We assume that the human importin-β 3D data used for the modeling is adequate because: (1) the size of human and *Drosophila* importin-βs are similar: 876 and 884 amino acids; (2) amino acid sequences of human and *Drosophila* importin-βs share 60% amino acid identity and 78% similarity (Lippai et al., 2000); and (3) The 10B HEAT repeat–linker–11A HEAT repeat region is evolutionary highly conserved: the amino acid identity and similarity are 64.1% and 92.3% (Table 3). Pro446 resides in the linker region between the B helix of HEAT repeat 10 and the A helix of HEAT repeat 11 at the beginning of a small 3-amino-acid-long α-helix after HEAT repeat 10 (Fig. 9) (Cingolani et al., 1999). CD spectra of model peptides representing the wild-type and the P446L mutant proteins reveal loss of flexibility upon Pro446→Leu replacement and the lost flexibility is most likely the consequence of the B helix of HEAT repeat 10 fusing with the short α helix in the linker region. Changing the Ψ and Φ angles of Leu439 and Leu440 such that the two amino acids fit into a fused α-helix, an open molecular conformation emerges (Fig. 9). As a consequence of opening the Spanish collar, the hydrophobic internal surface of the molecule becomes exposed to water. The consequence of the amino acid exchange may be less dramatic in the whole molecule due to its flexibility, but a significant conformational change is supported by the more hydrophobic behavior of the P446L mutant protein (i.e. it was much more difficult to express and purify compared with normal importin-β), and by the fact that the exchange of a distantly located residue suppresses the mutant defects caused by the P446L protein (see below).

S317T is an intragenic dominant suppressor mutation of *P446L* and restores *Ketel* gene function

Following molecular analysis of the *ketel*^{r} alleles, which are revertant alleles of the *Ketel*^{D} mutations and were induced

Table 3. Comparison of the amino acid sequence of the HEAT repeat 10 helix B–linker–HEAT repeat 11 helix A region of importin-β in different species

Species	Helix A of HEAT 10	Linker	Helix B of HEAT 11
Human	VVVRDTAAWTVGRICELL	**P**	EAAINDVYLAPLLQCLIEGL
Rat	VVVRDTTAWTVGRICELL	**P**	EAAINDVYLAPLLQCLIEGL
Drosophila	VIVRDTIAWTFGRICDII	**P**	EAAINETYLQTLLECFVKSL

P446, which is replaced by Leu in the P446L mutant protein, is highlighted in bold.

The identity and the similarity levels for the depicted region between human and *Drosophila* are 24/39 and 36/39.

The sources are as follows: human (Görlich et al., 1995), accession L38951, NID G893287; rat (Radu et al., 1995), accession L38644; *Drosophila* (Lippai et al., 2000), accession number AJ002729.

through second mutagenesis (Szabad et al., 1989; Erdélyi et al., 1997), we identified *S317T*, which is an intragenic dominant suppressor mutation of *P446L*. The *S317T* mutation originated through a single T→A transversion in the 3656th position and led to replacement of Ser317 by threonine. We generated five transgenic lines (labeled $K^{S317T\&P446L}$), which included both the *S317T* and the *P446L* mutations. The +/+; $K^{S317T\&P446L}$ females with two wild-type *Ketel* alleles (+) and with the $K^{S317T\&P446L}$ transgene are fully fertile, which suggests that the *S317T* mutation annulled the *P446L*-imposed dominant female sterility. That the $K^{S317T\&P446L}$ transgene does indeed restore *Ketel* gene function is best shown by the fact that the $ketel^{null}/-$; $K^{S317T\&P446L}$ zygotes are fully viable and fertile.

Discussion

Proline 446 is a functionally important residue in importin-β

The fact that in three of the four independently isolated $Ketel^{D}$ mutations the same C→T transition and the concurrent replacement of Pro446 by Leu is the basis of dominant female sterility underlines the importance of Pro446 in importin-β function. It is assumed that during a nuclear import cycle, whereas importin-β interacts with the NLS containing protein (directly or through importin-β), nucleoporins and RanGTP, the conformation of importin-β changes significantly (Vetter et al., 1999; Lee et al., 2000). In fact the region around HEAT repeat 10 was suggested, based on X-ray crystallography, to be a flexible point during switching between the IBB- and the Ran-bound forms. Pro446 resides in the linker region connecting HEAT repeats 10 and 11 and, as described here, plays a crucial role in enduring flexibility of importin-β. CD spectra of model peptides representing the wild-type and the P446L mutant proteins reveal loss of flexibility upon Pro446→Leu replacement. The lost flexibility is most likely the consequence of fusion of the small α-helix in the linker region with the α-helix of HEAT 10B. Computer 3D modeling of the P446L protein structure, based on results of CD spectroscopy, shows altered molecular structure: the P446L molecule takes on an open conformation such that its inner hydrophobic surface becomes exposed to water (compare Fig. 9B and D), explaining the reduced hydrophilic nature of the P446L protein.

The significant conformational change due to the exchange of Pro446 to Leu in the Ketel protein is further supported by the S317T suppressor mutation that restores *Ketel* gene function. In human importin-β the corresponding Ser311 (in the linker region between HEAT repeats 7 and 8) and Pro441 are 32.5 Å apart and yet the Ser→Thr exchange in the *Drosophila* homologue restores function of importin-β (Fig. 9). The 10 Å area surrounding serine is hydrophobic. The stronger hydrophobicity of threonine compared with serine does perhaps increase apolar interactions and bend the molecule back to its functional structure.

The P446L mutation changes Ran binding ability

Experiments with digitonin-permeabilized HeLa cells show that, to a reduced extent, the P446L proteins do participate in formation of the nuclear import complexes and in their docking to the cytoplasmic surface of the NE; however, they do not support import of the complexes into the nuclei in the presence of Ran, energy source, RanGAP and RanBP1. In fact, the import complexes do not form upon the addition of the latter components. Apparently the main structural domains of the P446L protein are intact (binds importin-α, NPC and Ran) but the interaction with Ran is altered. Indeed, we found that the binding of wild-type and P446L Ketel proteins to Ran are very different: the P446L cannot bind to RanGTP, to which the wild-type importin-β binds strongly, but shows elevated affinity to RanGDP, to which the wild-type protein shows very little affinity. It is noteworthy that a single amino acid exchange outside the classical Ran-binding domain can change Ran binding ability dramatically. The change in Ran-binding ability is most likely the source of the $Ketel^{D}$-associated dominant female sterility. However, the $Ketel^{D}$-associated dominant-negative effect is not manifested via nuclear protein import but rather through the prevention of cleavage nuclei formation: revealing a novel importin-β function.

The P446L mutant importin-β exerts its toxic effect at the end of mitosis

The injection experiments into wild-type cleavage embryos revealed that the P446L mutant protein does not inhibit nuclear protein import: when co-injected with P446L, a fluorescent nuclear substrate readily entered the nuclei. Furthermore, although the cleavage nuclei enter mitosis and the chromosomes segregate normally, intact NE never forms in the presence of P446L mutant importin-β. Failure of NE assembly in the presence of P446L is revealed by the following observations. First, the homogenous distribution of (1) a fluorescent nuclear substrate; (2) the high molecular weight dextrane; and (3) the GFP-tubulin. Second, the absence of the nuclear lamina lining. Thus the mutant P446L importin-β reveals a novel importin-β function required during the mitosis-to-interphase transition, a function distinct from the already known functions of importin-β in nuclear protein import and in mitotic spindle assembly (Görlich and Kutay, 1999; Wiese et al., 2001; Nachury et al., 2001; Gruss et al., 2001).

The P446L mutant importin-β possesses altered Ran-binding properties: it does not bind RanGTP but shows elevated affinity to RanGDP. A series of experiments showed that altered RanGTP-RanGDP balance leads to a similar phenotype in yeast (i.e. arrest in mitosis-to-interphase transition) (Sazer and Nurse, 1994; He et al., 1998). Results of enzyme assays described in the present paper show that the altered Ran-binding ability of P446L importin-β does not interfere with the GTP hydrolysis and nucleotide exchange on Ran and thus it is unlikely that the $Ketel^{D}$-related defects are consequences of distorted Ran metabolism. Most probably importin-β is a downstream effector of Ran during mitosis-to-interphase transition, as in nuclear protein import and mitotic spindle assembly.

Although several functions of Ran and importin-β during the cell cycle were described, the exact molecular mechanisms are still missing. Here we describe a novel function of *Drosophila* importin-β during mitosis-to-interphase transition where it is involved in the formation of intact NE. There seem to be three feasible explanations for the P446L-associated defects. First,

since the P446L importin-β shows higher affinity to RanGDP than wild-type importin-β, a possible explanation may be the depletion of significant amounts of RanGDP that is required for NE reassembly at the end of mitosis (Zhang and Clarke, 2000; Hetzer et al., 2000). Removal of RanGDP by P446L may lead to the failure of cleavage nuclei formation. We do not think this explanation is very likely for the following reasons. (1) Binding and nucleotide exchange assays revealed that the affinity of the P446L to RanGDP is low and hence depletion of a significant fraction of Ran from the cytoplasm is rather unlikely. (2) Interestingly, defects do not evolve in nuclear protein import or in spindle formation and chromosome segregation following injection of P446L despite the fact that both nuclear protein import and spindle formation have been shown to be Ran dependent. Ran's involvement in NE assembly has also been described but since none of the aforementioned Ran-related processes were disturbed, the P446L protein does not seem to disturb the Ran cycle. A second possible explanation of the P446L-related defects is perhaps the inability of the P446L protein to bind RanGTP and, consequently, the inability to release factors required for proper chromatin decondensation and/or NE assembly. In this case the role of importin-β in the above processes would resemble its function in mitotic spindle formation, where it is thought to be required for the release of factors needed for spindle assembly [e.g. NuMA, TPX2 (Wiese et al., 2001; Nachury et al., 2001; Gruss et al., 2001)]. A third possibility is that the P446L-related defects are not associated with the change in Ran-binding ability. The *P446L* mutation may disturb the association of thus far unidentified factors (e.g. nucleoporins). In the case of the second and third possibilities the factor(s) required for the newly described importin-β-related functions remain to be identified.

We thank Révész Kati and Kissné Ani for their excellent technical help. We are grateful to F. Nagy for his laboratory facilities in sequencing the *Ketel*^{D1} allele. We thank D. Görlich for his generous supply of the Ran mixture and the fluorescein-labeled IBB core pentamer; B. Ganetzky for the *Drosophila* RanGAP expression vector; M. Frasch for the anti-dRan antibody; and N. Stuurman for the lamin-GFP transgene-carrying strains. We thank W. Moore, C. Zhang and Z. Gáspári for their help in the enzymatic and binding assays and in recording the CD spectra, respectively. Support for the 'Ketel project' came from several sources: OTKA 992, OTKA T5537, OTKA 32540 from the Hungarian National Science Foundation, FKFP grant 1348/1997 from the Hungarian Education and Science Foundation, the PHARE-ACCORD Program No. H-9112-0528 and the PECO No. CEC ERB CIPD CT 94 0049 EC Cell Cycle Network program organized by David Glover. The work in Dundee was supported by an EMBO Short Term Fellowship ASTF 9824 to L.T.

References

Adam, S. A., Marr, R. S. and Gerace, L. (1990). Nuclear protein import in permeabilized mammalian cells requires soluble cytoplasmic factors. *J. Cell Biol.* **111**, 807-816.

Azuma, Y. and Dasso, M. (2000). The role of Ran in nuclear function. *Curr. Opin. Cell Biol.* **12**, 302-307.

Bischoff, F. R. and Görlich, D. (1997). RanBP1 is crucial for the release of RanGTP from importin beta-related nuclear transport factors. *FEBS Lett.* **419**, 249-254.

Cingolani, G., Petosa, C., Weis, K. and Muller, C. W. (1999). Structure of importin-β bound to the IBB domain of importin-β. *Nature* **399**, 221-229.

Clarkson, M. and Saint, R. (1999). A His2AvDGFP fusion gene complements a lethal His2AvD mutant allele and provides an in vivo marker for *Drosophila* chromosome behavior. *DNA Cell Biol.* **18**, 457-462.

Erdélyi, M., Máthé, E. and Szabad, J. (1997). Genetic and developmental analysis of mutant Ketel alleles that identify the *Drosophila* importin-β homologue. *Acta Biol. Hung.* **48**, 323-338.

Erdélyi, M. and Szabad, J. (1989). Isolation and characterization of dominant female sterile mutations of *Drosophila melanogaster*. I. Mutations on the third chromosome. *Genetics* **122**, 111-127.

Foe, V. E., Odell, G. M. and Edgar, B. A. (1993). Mitosis and morphogenesis in the *Drosophila* embryo: point and counterpoint. In *The Development of Drosophila melanogaster* (ed. M. Bate and A. Martinez-Arias), pp. 149-300. New York: Cold Spring Harbor Laboratory Press.

Görlich, D. and Kutay, U. (1999). Transport between the cell nucleus and the cytoplasm. *Annu. Rev. Cell Dev. Biol.* **15**, 607-660.

Görlich, D., Pante, N., Kutay, U., Aebi, U. and Bischoff, F. R. (1996). Identification of different roles for RanGDP and RanGTP in nuclear protein import. *EMBO J.* **15**, 5584-5594.

Grieder, N. C., de Cuevas, M., Spradling, A. C. (2000). The fusome organizes the microtubule network during oocyte differentiation in *Drosophila*. *Development* **127**, 4253-4264.

Gruss, O. J., Carazo-Salas, R. E., Schatz, C. A., Guarguaglini, G., Kast, J., Wilm, M., Le Bot, N., Vernos, I., Karsenti, E. and Mattaj, I. W. (2001). Ran induces spindle assembly by reversing the inhibitory effect of importin-β on TPX2 activity. *Cell* **104**, 83-93.

He, X., Hayashi, N., Walcott, N. G., Azuma, Y., Patterson, T. E., Bischoff, F. R., Nishimoto, T. and Sazer, S. (1998). The identification of cDNAs that affect the mitosis-to-interphase transition in *Schizosaccharomyces pombe*, including *shp1*, which encodes a spi1p-GTP–binding protein. *Genetics* **148**, 645-656.

Hetzer, M., Bilbao-Cortes, D., Walther, T. C., Gruss, O. J. and Mattaj, I. W. (2000). GTP hydrolysis by Ran is required for nuclear envelope assembly. *Mol. Cell* **5**, 1013-1024.

Hughes, M., Zhang, C., Avis, J. M., Hutchins, C. J. and Clarke, P. R. (1998). The role of the ran GTPase in nuclear assembly and DNA replication: characterisation of the effects of Ran mutants. *J. Cell Sci.* **111**, 3017-3026.

Kutay, U., Izaurralde, E., Bischoff, F. R., Mattaj, I. W. and Görlich, D. (1997). Dominant-negative mutants of importin-β block multiple pathways of import and export through the nuclear pore complex. *EMBO J.* **16**, 1153-1163.

Lee, S. J., Imamoto, N., Sakai, H., Nakagawa, A., Kose, S., Koike, M., Yamamoto, M., Kumasaka, T., Yoneda, Y. and Tsukihara, T. (2000). The adoption of a twisted structure of importin-β is essential for the protein-protein interaction required for nuclear transport. *J. Mol. Biol.* **302**, 251-264.

Lindsley, D. L. and Zimm, G. G. (1992). The Genome of *Drosophila melanogaster*. San Diego and London: Academic Press.

Lippai, M., Tirián, L., Boros, I., Mihály, J., Erdélyi, M., Belecz, I., Máthé, E., Pósfai, J., Nagy, A., Udvardy, A. et al. (2000). The *Ketel* gene encodes a *Drosophila* homologue of importin-β. *Genetics* **156**, 1889-1900.

Mattaj, I. W. and Englmeier, L. (1998). Nucleocytoplasmic transport: the soluble phase. *Annu. Rev. Biochem.* **67**, 265-306.

Melchior, F. and Gerace, L. (1998). Two-way trafficking with Ran. *Trends Cell Biol.* **8**, 175-179.

Merrifield, R. B. (1963). The synthesis of a tetrapeptide. Solid phase peptide synthesis. *J. Am. Chem. Soc.* **85**, 2149-2154.

Nachury, M. V., Maresca, T. J., Salmon, W. C., Waterman-Storer, C. M., Heald, R. and Weis, K. (2001). Importin-β is a mitotic target of the small GTPase Ran in spindle assembly. *Cell* **104**, 95-106.

Paddy, M. R., Saumweber, H., Agard, D. A. and Sedat, J. W. (1996). Time-resolved in vivo studies of mitotic spindle formation and nuclear lamina breakdown in *Drosophila* early embryos. *J. Cell Sci.* **109**, 591-607.

Pemberton, L. F., Blobel, G. and Rosenblum, J. S. (1998). Transport routes through the nuclear pore complex. *Curr. Opin. Cell Biol.* **10**, 392-399.

Perczel, A., Hollósi, M., Tusnády, G. and Fasman, G. D. (1991). Convex constraint analysis: a natural deconvolution of circular dichroism curves of proteins. *Protein Eng.* **4**, 669-679.

Perczel, A., Park, K. and Fasman, G. D. (1992). Analysis of the circular dichroism spectrum of proteins using the convex constraint algorithm: a practical guide. *Anal. Biochem.* **203**, 83-93.

Radu, A., Blobel, G. and Moore, M. S. (1995). Identification of a protein complex that is required for nuclear protein import and mediates docking of import substrate to distinct nucleoporins. *Proc. Natl. Acad. Sci. USA* **92**, 1769-1773.

Reuter, G. and Wolff, I. (1981). Isolation of dominant suppressor mutations for position-effect variegation in *Drosophila melanogaster*. *Mol. Gen. Genet.* **182**, 516-519.

Sazer, S. and Nurse, P. (1994). A fission yeast RCC1-related protein is required for the mitosis to interphase transition. *EMBO J.* **13**, 606-615.

Szabad, J., Erdélyi, M., Hoffmann, G., Szidonya, J. and Wright, T. R. F. (1989). Isolation and characterization of dominant female sterile mutations of *Drosophila melanogaster*. II. Mutations on the second chromosome. *Genetics* **122**, 823-835.

Thummel, C. S., Boulet, A. M. and Lipshitz, H. D. (1988). Vectors for *Drosophila* P-element-mediated transformation and tissue culture transfection. *Gene* **74**, 445-456.

Timmons, L., Hersperger, E., Woodhouse, E., Xu, J., Liu, L. Z. and Shearn, A. (1993). The expression of the *Drosophila* awd gene during normal development and in neoplastic brain tumors caused by *lgl* mutations. *Dev. Biol.* **158**, 364-379.

Tirián, L., Puro, J., Erdélyi, M., Boros, I., Papp, B., Lippai, M. and Szabad, J. (2000). The *Ketel*^{D} dominant-negative mutations identify maternal function of the *Drosophila* Importin-β gene required for cleavage nuclei formation. *Genetics* **156**, 1901-1912.

Van Doren, M., Williamson, A. L. and Lehmann, R. (1998). Regulation of zygotic gene expression in *Drosophila* primordial germ cells. *Curr. Biol.* **8**, 243-246.

Vetter, I. R., Arndt, A., Kutay, U., Görlich, D. and Wittinghofer, A. (1999). Structural view of the Ran-importin-β interaction at 2.3 Å resolution. *Cell* **97**, 635-646.

Weis, K. (1998). Importins and exportins: how to get in and out of the nucleus. *Trends Biochem. Sci.* **23**, 185-189.

Wiese, C., Wilde, A., Moore, M. S., Adam, S. A., Merdes, A. and Zheng, Y. (2001). Role of importin-β in coupling Ran to downstream targets in microtubule assembly. *Science* **291**, 653-656.

Wozniak, R. W., Rout, M. P. and Aitchison, J. D. (1998). Karyopherins and kissing cousins. *Trends Cell Biol.* **8**, 184-188.

Zhang, C. and Clarke, P. R. (2000). Chromatin-independent nuclear envelope assembly induced by Ran GTPase in Xenopus egg extracts. *Science* **288**, 1429-1432.

P446L-importin-β inhibits nuclear envelope assembly by sequestering nuclear envelope assembly factors to the microtubules

László Tirián[2], Gyula Timinszky[2], János Szabad[1]

The University of Szeged, Faculty of Medicine, Department of Biology, Szeged/Hungary

Received October 9, 2002
Received in revised version February 5, 2003
Accepted March 19, 2003

Importin-β – nuclear envelope – Ran – microtubules – Drosophila mutant

The P446L mutant *Drosophila* importin-β (P446L-imp-β) has been reported to prohibit – in dominant negative fashion – nuclear envelope (NE) assembly. Along elucidating the mode of action of P446L-imp-β we studied in vitro NE assembly on Sepharose beads. While *Drosophila* embryo extracts support NE assembly over Sepharose beads coated with Ran, NE assembly does not take place in extracts supplied with exogenous P446L-imp-β. A NE also forms over importin-β-coated beads. Surprisingly, when immobilized to Sepharose beads P446L-imp-β as efficiently recruits NE vesicles as normal importin-β. The discrepancy in behavior of cytoplasmic and bead-bound P446L-imp-β appears to be related to icreased – as compared to normal importin-β – microtubule (MT) binding ability of P446L-imp-β. While wild-type importin-β is able to bind MTs and the binding decreases upon RanGTP interaction, P446L-imp-β cannot be removed from the MTs by RanGTP. P446L-imp-β, like normal importin-β, binds some types of the nucleoporins that have been known to be required for NE assembly at the end of mitosis. It appears that the inhibitory effect of P446L-imp-β on NE assembly is caused by sequestering some of the nucleoporins required for NE assembly to the MTs.

Abbreviations. BSA Bovine serum albumin. – DHCC 3,3′-Dihexyloxacarbocyanine iodide. – MAP Microtubule-associated protein. – MT Microtubule. – NE Nuclear envelope. – NPC Nuclear pore complex. – Nup Nucleoporin. – P446L-imp-β P446L mutant *Drosophila* importin-β. – RanBP1 Ran-binding protein 1. –RanGAP Ran GTPase-activating protein. – RCC1 Regulator of chromatin condensation 1. – NTF2 Nuclear translocation factor 2.

[1] Dr. János Szabad, The University of Szeged, Faculty of Medicine, Department of Biology, Somogyi u. 4, H-6720 Szeged/Hungary, e-mail: szabad@mdbio.szote.u-szeged.hu, Fax: +36 62 54 5131.
[2] These authors contributed equally to this work.

Introduction

Importin-β has important functions throughout the cell cycle. It is (*i*) an important component of nuclear protein import (Gorlich and Kutay, 1999), (*ii*) plays a role in mitotic spindle formation (Gruss et al., 2001; Nachury et al., 2001; Wiese et al., 2001) and (*iii*) was recently shown to be involved in NE assembly (Timinszky et al., 2002; Zhang et al., 2002). It is generally accepted that Ran regulates importin-β function in all three processes. The regulatory effects of Ran are best characterized in nuclear protein import. In brief, while the GDP-bound form of Ran cannot, the GTP-bound form of Ran binds importin-β. When importin-β is not associated with RanGTP it is able to bind cargo molecules to be imported into the nucleus, interact with nucleoporins (Nups), nuclear pore complex (NPC) proteins and translocate through the NPCs. Following interaction with RanGTP in the nucleus importin-β releases its cargo. Importin-β is subsequently exported from the nucleus and – through interactions with RanGAP and RanBP1 – hydrolyzes RanGTP to become free to initiate the next nuclear protein import cycle (Görlich and Kutay, 1999). The asymmetric distribution of the proteins regulating the RanGTPase cycle leads to a steep RanGTP gradient across the NE that is the driving force for nuclear protein import: while RCC1, the only known guanine nucleotide exchange factor for Ran, is chromatin bound, RanGAP and RanBP1 are cytoplasmic. Ran regulates importin-β function in a similar way during mitotic spindle formation by releasing the importin-β-bound MT assembly-promoting factors in the vicinity of chromatin where the chromatin associated RCC1 creates a high RanGTP concentration. It was furthermore shown recently that RanGTP is concentrated over the mitotic spindle in cleavage *Drosophila* embryos (Trieselmann and Wilde, 2002). The process of NE assembly over the segregating chromosomes is still not very well understood. Presence of a number of proteins has been shown to be required for NE assembly (for a review see (Burke and Ellenberg, 2002)): Ran with its regulators, p97-

0171-9335/03/82/0■-1 $15.00/0

AAA ATPase with associated factors, several Nups, components of the nuclear lamina as well as importin-β.

When immobilized to Sepharose beads importin-β – just like Ran – recruits NE vesicles and induces NE assembly. When, however, those amino acids are changed in importin-β that are engaged in interaction with the FxFG motifs of the nucleoporins (Phe-x-Phe-Gly, where x is usually Ser, Gly, or Ala), the mutant importin-β cannot recruit NE vesicles and facilitate NE assembly over the Sepharose beads (Zhang et al., 2002). Thus importin-β is believed to be involved in NE assembly by recruiting NE vesicles to the chromatin.

Ketel, the *Drosophila* homologue of importin-β was identified by four dominant female sterile (*Ketel^D*) mutations causing (*i*) NE defects and (*ii*) the formation of giant and persisting sperm aster microtubules following fertilization (Tirian et al., 2000). In three of the four independently isolated *Ketel^D* mutations the same base pair substitution mutation leads to replacement of Pro^{446} by Leu (P446L-imp-β) and the formation of a highly toxic protein that induces death when injected into wild-type embryos (Tirian et al., 2000; Timinszky et al., 2002). P446L-imp-β does not exert its dominant negative effect through (*i*) blocking nuclear protein import neither in cleavage *Drosophila* embryos nor in digitonin-permeabilized HeLa cells, or (*ii*) through preventing mitotic spindle formation and chromosome segregation as was demonstrated by injection into cleavage embryos expressing tubulin-GFP or histone-GFP (Timinszky et al., 2002). It appears that P446L-imp-β induces death of the *Drosophila* embryos by preventing NE reassembly at the end of mitosis as indicated by (*i*) the failure of nuclear lamina assembly and (*ii*) the observation that macromolecules are not excluded from the presumptive sites of the "nuclei". It has also been established that P446L-imp-β – though the amino acid replacement resides in the presumptive nucleoporin- and importin-α-binding domain of importin-β – does interact with both importin-α and nucleoporins since P446L-imp-β can dock nuclear proteins to NPCs in the absence of Ran in digitonin-permeabilized HeLa cells. But unlike normal importin-β, P446L-imp-β cannot bind RanGTP. The explanation of the unusual behavior of P446L-imp-β stems most likely from a large conformational change in the molecule upon replacement of the helix-breaking proline to leucine (Timinszky et al., 2002). We set out to study the mode of P446L-imp-β action and understand – in light of P446L-imp-β function – novel aspects of NE formation. In the present report we show that P446L-imp-β blocks NE assembly over Ran-coated Sepharose beads but can recruit NE vesicles and some Nups when immobilized to Sepharose beads. It appears that the inhibitory effect of P446L-Imp-β on NE assembly stems from its altered RanGTP-binding ability and the consequent cytoplasmic mislocalization on MTs. Here we show evidence that wild-type importin-β can bind the MTs both directly and indirectly through binding some types of the microtubule-associated proteins (MAPs). MT binding in both cases decreases upon importin-β RanGTP interaction. P446L-imp-β binds MTs with higher affinity than normal importin-β and because P446L-imp-β does not bind RanGTP it remains attached to MTs and sequesters some types of the Nups required for NE assembly.

Materials and methods

Recombinant proteins and immunostaining

Wild-type and P446L-imp-β were produced and purified as described in (Lippai et al., 2000; Timinszky et al., 2002). Importin-β and tubulin were detected in digitonin-permeabilized HeLa cells – following a 3% paraformaldehyde fixation – by affinity-purified anti-Ketel primary antibody (Lippai et al., 2000) and an anti-tubulin monoclonal antibody DM 1A (Sigma) and FITC- and Texas Red-conjugated secondary antibodies (Jackson Laboratories), respectively.

In vitro nuclear envelope assembly

NE assembly around RanGDP-loaded glutathione-Sepharose beads or protein A-Sepharose beads loaded with anti-Ketel antibody was monitored following staining with 3,3'-dihexyloxacarbocyanine iodide (DHCC, a fluorescent dye that labels phospholipid membranes) or immunostaining with the monoclonal anti-nucleoporin antibody mAb414 (BAbCO) as described in (Zhang and Clarke, 2000) with the following modifications: Extracts from *Drosophila* embryos (0–3 hours old) were prepared by dechorionating the eggs in Clorox and thoroughly rinsing in KHM buffer on ice (Zhang and Clarke, 2001). The eggs were either immediately homogenized or frozen in liquid nitrogen. After homogenization the procedure was identical to that described for the preparation of HeLa cell extract (Zhang and Clarke, 2001).

To prepare importin-β- and P446L-imp-β-coated beads, we loaded protein A-Sepharose beads with anti-Ketel antibody by incubating 60 µl of beads in 500 µl KHM solution containing ~50 µg/ml affinity-purified anti-Ketel polyclonal antibody for 2 hours at room temperature on a rotating platform. When indicated the beads were loaded with wild-type importin-β or with P446L-imp-β by an overnight incubation of 50 µl anti-Ketel-loaded protein A-Sepharose beads in 500 µl KHM solution containing 3 µM importin-β. The beads were washed several times in KHM buffer and stored frozen at −70°C.

Images were taken either in a Zeiss Axiovert fluorescence microscope with a cooled CCD camera or with a Zeiss Axiovert confocal microscope. Images were processed either with Improvision Openlab and Adobe Photoshop software or Zeiss LSM and Corel Photopaint software.

In vitro tubulin binding assay

Microtubule preparation was carried out according to Cullen et al. (1999) with some modifications. *Drosophila* whole extracts were prepared from female fruit flies fed for 3 days to be at the top of their egg laying period to obtain the biggest ovary to body ratio. Flies were homogenized in PEM buffer (50 mM Pipes, pH 6.8, 5 mM EGTA, 5 mM $MgSO_4$) containing a cocktail of protease inhibitors and 1 mM dithiothreitol. The homogenate was incubated at 0°C for 30 minutes and spun at 120000*g* at 4°C for 30 minutes. Taxol (paclitaxel, Sigma) (final concentration 20 µM) and tubulin (final concentration 10 µM) and – if mentioned – RanQ69L (final concentration 3 µM) were added to the supernatant before incubation at 36°C for 30 minutes to polymerize microtubules. The microtubules and associated proteins were pelleted by spinning at 80000*g* at 36°C for 30 minutes through a 30% sucrose cushion in PEM buffer.

In an other set of experiments a final concentration of 10 µM tubulin and 20 µM taxol in PEM buffer containing 1 µg/ml BSA was used at 36°C for 30 minutes to polymerize microtubules. Before the incubation period recombinant proteins were added to the tubulin solution when mentioned. A final concentration of 0.5 µM importin-β and 3 µM RanQ69L or RanGDP was used. The microtubules and associated proteins were pelleted by spinning at 80000*g* at 36°C for 30 minutes through a 30% sucrose cushion in PEM buffer.

The supernatant and pellet fractions were analyzed by SDS-polyacrylamide gel electrophoresis and Western blotting. The proteins were detected by an ECL Western blotting kit (Amersham Pharmacia) using a Molecular Probes Typhoon 8600 optical scanner, and the bands were analyzed using Molecular Probes ImageQuant 5.2 software.

Results

P446L-imp-β inhibits NE assembly over Ran coated Sepharose beads

Ran bound to Sepharose beads initiates the assembly of functional NE in vitro not only in extracts of *Xenopus* eggs (Zhang and Clarke, 2000) or mammalian mitotic cells (Zhang and Clarke, 2001) but also in extracts of wild-type *Drosophila* embryos. In fact the *Drosophila* wild-type embryo extract supports NE assembly around the Ran-coated beads as efficiently as the *Xenopus* egg extract: NE assembled within 60 minutes as revealed by the fluorescent halo around the beads (Fig. 1a). However, when the Ran-coated beads were incubated in *Ketel*^{D} egg extracts, NE did not form even during a two-hour incubation period (Fig. 1a). (The *Ketel*^{D} eggs were deposited by the *Ketel*^{D}/+ heterozygous females; Tirian et al., 2000.) When 3 μM exogenous wild-type *Drosophila* importin-β was added (to reach the importin-β concentration in *Xenopus* eggs) to the wild-type *Drosophila* embryo extract, complete NE assembled within 15 minutes (Fig. 1b). To test the dominant negative effect of P446L-imp-β on NE assembly, we incubated Ran-coated Sepharose beads in wild-type extracts into which 3 μM purified P446L-imp-β had been added. P446L-imp-β prevented NE formation (Fig. 1b). The above experiments demonstrated that (*i*) wild-type *Drosophila* embryo extracts support NE assembly in vitro around Ran-coated Sepharose beads, (*ii*) wild-type importin-β accelerates NE assembly and (*iii*) P446L-imp-β – either in extracts of the *Ketel*^{D} eggs or exogenously added to wild-type extracts – blocks NE assembly in dominant negative fashion. Thus results of these in vitro experiments are in agreement with the in vivo experiments described in (Tirian et al., 2000; Timinszky et al., 2002).

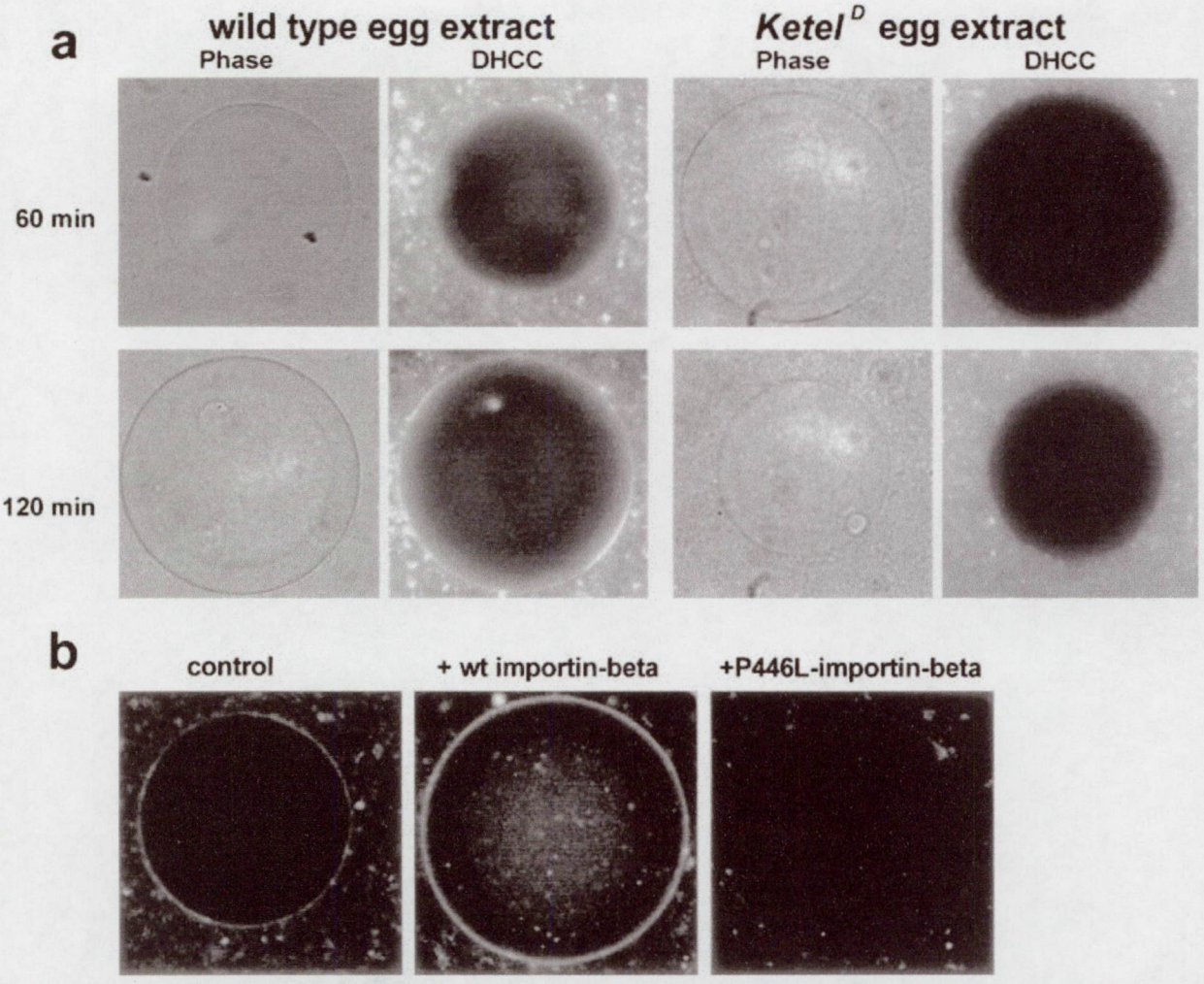

Fig. 1. Effect of the *Ketel*^{D}-encoded P446L-imp-β on NE assembly around Ran-coated Sepharose beads. Glutathione-Sepharose beads were loaded with RanGDP and incubated in extract prepared from *Drosophila* embryos (0–3 hours old). After 60 or 120 minutes of incubation the samples were diluted 20-fold by PBS and stained with the membrane-labeling dye DHCC. The beads were examined in either a fluorescence (**a**) or a confocal (**b**) microscope. (**a**) The bright halo around the beads indicates NE assembly around the bead. Note that NE assembly did not occur in *Ketel*^{D} egg extracts even during 120 minutes. (**b**) While the addition of wild-type *Drosophila* importin-β facilitated NE assembly in the wild-type egg extract, the mutant P446L-imp-β inhibited NE assembly.

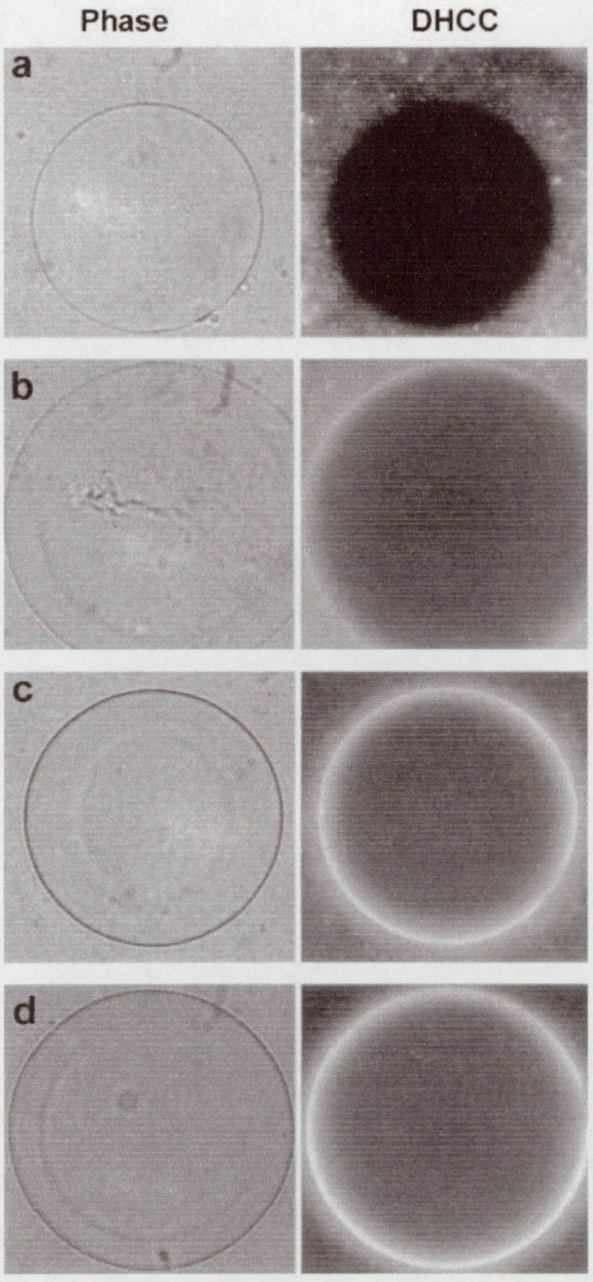

Fig. 2. NE assembly around wild-type importin-β- and P446L-imp-β-coated beads. Beads with different types of coats were incubated for ten minutes in extract prepared from wild-type *Drosophila* embryos and stained with DHCC for the presence of NE. NE assembly does not occur over protein A-coated (control) Sepharose beads (**a**), but over beads coated with anti-Ketel antibody (**b**). High amounts of NE materials assemble over beads coated with wild-type *Drosophila* importin-β (**c**) or P446L-imp-β (**d**).

NE assembly over importin-β-coated Sepharose beads

It was shown recently that NE assembly occursover importin-β-coated Sepharose beads in *Xenopus* egg extract (Zhang et al., 2002). It was revealed furthermore that Sepharose beads coated with the 45–462 truncated form of importin-β, which cannot bind RanGTP and importin-α but bind Nups, are capable of recruiting NE components, while Sepharose beads coated with I178D importin-β, which cannot bind Nups, are deficient in stimulating NE assembly (Zhang et al., 2002). To study whether P446L-imp-β is able to recruit NE components we coated the Sepharose beads with wild-type importin-β or with P446L-imp-β by (*i*) chemically coupling to BrCN-activated Sepharose and also (*ii*) through a polyclonal anti-Ketel antibody and protein A-Sepharose. Results of the two types of couplings were essentially identical. However, because the BrCN-activated Sepharose beads bind DHCC, and strong background fluorescence emerged, only results of the antibody coupling experiments are presented (Fig. 2). There was no NE assembly over the control protein A-Sepharose beads in extracts of wild-type *Drosophila* embryos (Fig. 2a). When, however, the protein A-Sepharose beads were coated with the anti-Ketel antibody NE assembly around the beads occurred within the first 10 minutes of incubation (Fig. 2b). NE assembly was even faster and more intensive over those protein A-Sepharose beads that had been coated with anti-Ketel antibody and preloaded with wild-type importin-β (Fig. 2c). The most likely explanation for the accelerated NE assembly – as compared to the Ran-coated beads – is the high importin-β concentration readily available over the bead surface such that the importin-β molecules can bind vesicles with NE components.

Identical results were obtained for beads preloaded with P446L-imp-β (Fig. 2d). This rather surprising result shows that – in contrast to the in vivo or in vitro experiments with Ran-coated beads where P446L-imp-β blocks NE assembly – it induces NE assembly when immobilized to the Sepharose beads.

We also determined whether the above-described beads recruited some of the nucleoporins by making use of the anti-nucleoporin antibody mAb414. Apparently, when immobilized to beads wild-type and P446L-imp-β molecules equally efficiently recruit nucleoporins as it appeared following immunostaining (Fig. 3) or Western blot analysis (data not shown). It should be noted that the mAb414-based staining was much more intensive over the importin-β-coated beads as compared with the Ran-coated beads (Fig. 3).

The mislocalization of P446L-imp-β on microtubules

A plausible explanation for the unexpected behavior of P446L-imp-β, i.e. it inhibits NE assembly in vivo and in vitro on Ran-coated Sepharose beads and yet supports NE assembly when directly bound to Sepharose beads, is that the P446L-imp-β molecules cannot localize correctly in the egg extract and also in the *Ketel*^{D} eggs. The dominant negative nature of P446L-imp-β becomes understandable if P446L-imp-β binds factors required for NE assembly (as shown by its ability to initiate NE formation when bound to the Sepharose beads) and sequesters them via mislocalization. To find out whether P446L-imp-β is indeed mislocalized inside the cells, we analyzed the distribution of wild-type and P446L-imp-β molecules in digitonin-permeabilized HeLa cells that are routinely used for analysis of nuclear protein import. (We could not use *Drosophila* embryos since there is a huge stockpile of maternally provided importin-β in the egg cytoplasm, a condition that does not allow detection of differences in importin-β distribution in wild-type and *Ketel*^{D} eggs (Lippai et al., 2000)). Following permeabilization by digitonin, the soluble cytoplasmic factors – including those involved in nuclear protein import – are washed away from the

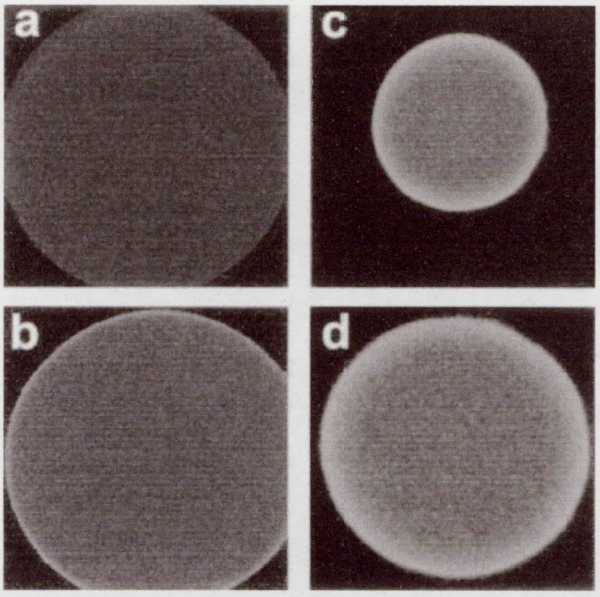

Fig. 3. Nucleoporins are embedded in the NE that forms over Sepharose beads coated with wild-type importin-β or P446L-imp-β. Beads with different types of coats were incubated for one hour in extract prepared from wild-type *Drosophila* embryos and immunostained with the anti-nucleoporin antibody mAb414. There is no indication of Nups over protein A-coated (control) Sepharose beads (**a**). The presence of Nups is apparent over Ran-coated beads (**b**). Along with the high amount of NE material (as shown in Fig. 2c, d), intensive Nup signal emerged from both the importin-β- (**c**) and the P446L-imp-β-coated beads (**d**).

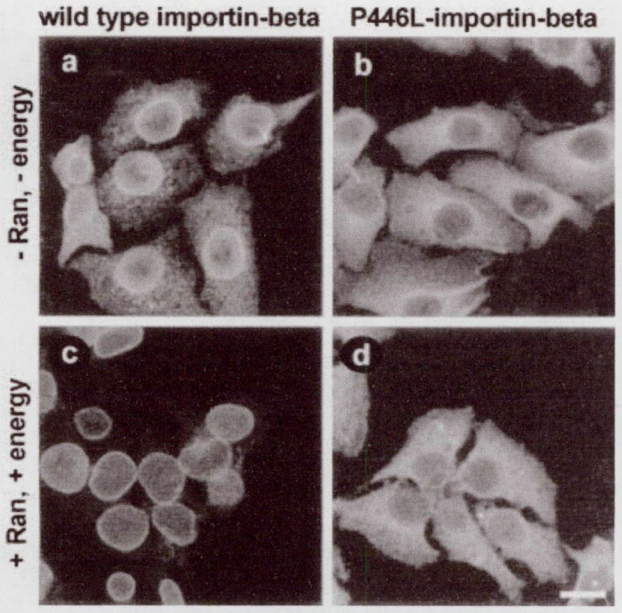

Fig. 4. The localization of wild-type importin-β and P446L-imp-β in digitonin-permeabilized HeLa cells. In the absence of a "Ran mixture" and an energy-regenerating system both wild-type importin-β (**a**) and P446L-imp-β (**b**) localize to the cytoplasm with slight accumulation over the NE. (The "Ran mixture" is composed from Ran, RanBP1, NTF2 and RanGAP.) In the presence of "Ran mixture" and an energy-regenerating system P446L-imp-β molecules remain cytoplasmic (**d**), while wild-type importin-β binds exclusively to the NE (**c**). Bar 10 μm.

HeLa cells. Nuclear protein import is analyzed following the re-addition of purified wild-type importin-β or P446L-imp-β along with other components of nuclear protein import. We used immunostaining to detect wild-type importin-β or P446L-imp-β in the digitonin-permeabilized HeLa cells. (It should be noted that the polyclonal anti-Ketel antibody equally efficiently recognizes wild-type importin-β and P446L-imp-β.) In the presence of nuclear protein and in the absence of Ran and an energy-regenerating system, wild-type importin-β and P446L-imp-β are uniformly distributed in the cytoplasm, although wild-type importin-β is slightly more abundant around the NE than P446L-imp-β (Fig. 4a, b). However, in the presence of Ran and an energy-regenerating system there is a major difference between the localization of wild-type and the P446L-imp-β molecules: while wild-type importin-β localizes exclusively to the NE (Fig. 4c), being engaged in nuclear protein import, P446L-imp-β is completely cytoplasmic, showing mislocalization of P446L-imp-β (Fig. 4d).

Since the cytoplasmic distribution pattern of importin-β and P446L-imp-β in digitonin-permeabilized HeLa cells was reminiscent of the MT cytoskeleton, we double stained digitonin-permeabilized HeLa cells with anti-Ketel and anti-tubulin antibodies and analyzed the cells in a confocal microscope. Results of the staining show localization of P446L-imp-β to MTs in the presence of RanGTP (Fig. 5).

To examine if there is a difference in MT-binding ability of wild-type importin-β and P446L-imp-β, cytoplasmic extracts were prepared from wild-type and $Ketel^{D}/+$ females. It should be mentioned that the cytoplasmic extracts of $Ketel^{D}/+$ females

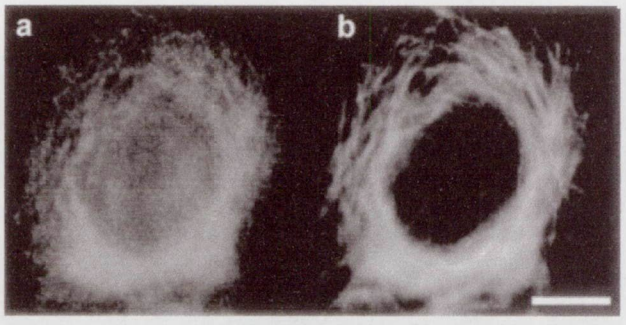

Fig. 5. P446L-imp-β co-localizes with MTs in digitonin-permeabilized HeLa cells. P446L-imp-β, "Ran mixture" and energy-regenerating system were added to digitonin-permeabilized HeLa cells, fixed after five-minute incubation and stained with anti-Ketel (**a**) and anti-tubulin (**b**) antibody. Note accumulation of P446L-imp-β over MTs. Bar 10 μm.

contain 50% wild-type importin-β and 50% P446L-imp-β. The extracts were supplemented with 10 μM tubulin to reach the critical concentration required for tubulin polymerization, and MT formation was induced by the addition of 20 μM taxol. Two conditions were examined. In the first one, no RanQ69L was added to the extract to mimic cytoplasmic conditions distant from chromatin. (RanQ69L is a GTP-loaded, GTPase-deficient mutant form of Ran.) In the second condition, RanQ69L was added to a final concentration of 3 μM to mimic conditions near chromatin where Ran exists in its GTP-bound state (Kalab

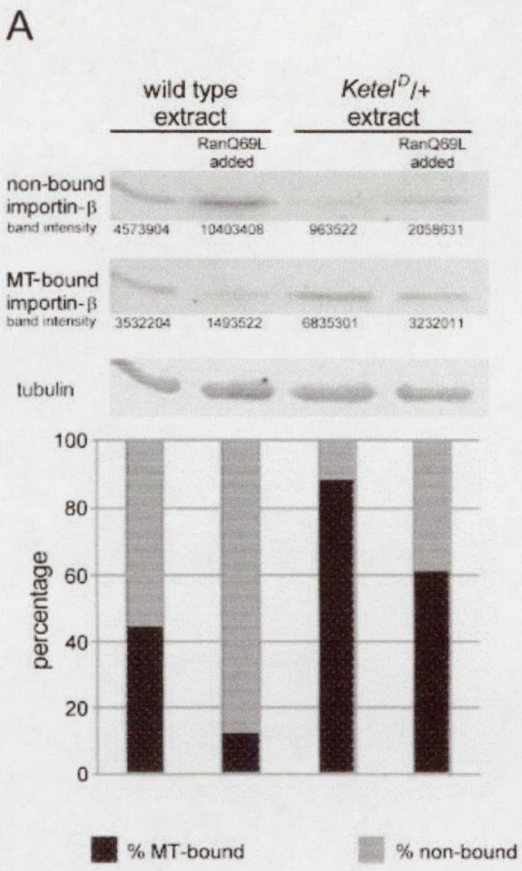

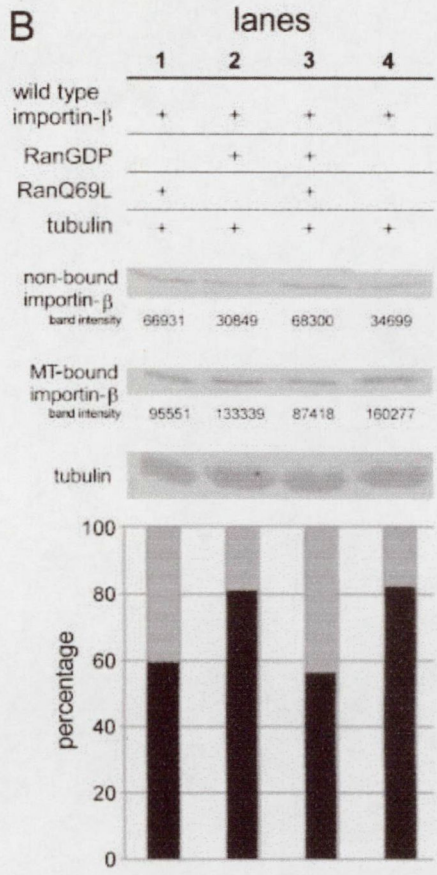

Fig. 6. In vitro assembled MTs pull down importin-β in a RanGTP-dependent way. MTs were polymerized in wild-type and *Ketel*^{D}/+ extracts (**A**) or in the presence of purified wild-type importin-β (**B**) under the conditions indicated and subsequently centrifuged through a 30% sucrose cushion. Importin-β in the supernatant and the MT pellet was detected by Western blot using anti-Ketel antibody. Polymerized MTs were detected using anti-tubulin antibody. The ratio of non-bound and MT-bound importin-β under different conditions was calculated by ImageQuant software and is shown in the bottom diagrams. Importin-β-MT interaction decreases in the presence of RanQ69L (**A**, **B**). Significantly more importin-β is bound to MTs in the *Ketel*^{D}/+ extract (**A**). The increased amount of importin-β is not merely the result of the inability of P446L-imp-β to bind RanGTP for more importin-β is bound to MTs in the *Ketel*^{D}/+ extract than in the wild-type extract even in the absence of RanQ69L (**A**); P446L-imp-β has higher MT-binding ability than wild-type importin-β.

et al., 2002). Addition of RanQ69L removed a significant amount of importin-β from MTs in both wild-type and *Ketel*^{D}/+ extracts (Fig. 6A). However, even in wild-type extract 12% of importin-β remained bound to MTs in the presence of RanQ69L. Thus MT-importin-β binding seems to originate from a RanGTP-sensitive pool and an -insensitive pool that may come from direct binding of importin-β to the MTs.

To investigate if importin-β does indeed bind MTs directly, MTs were polymerized in the presence of purified wild-type importin-β. (Results of the experiments with purified P446L-imp-β are not shown because it forms aggregates and is pelleted in the absence of MTs under the experimental conditions used.) If the reaction mixture contains only tubulin and wild-type importin-β, importin-β is present exclusively together with the pelleted MTs irrespective of being alone or together with RanGDP or RanQ69L (data not shown). When the mixture is supplied with 1 mg/ml BSA, 82% of importin-β appears in the pellet bound to MTs (Fig. 6B). (BSA does not bind to MTs under any conditions examined and no importin-β was found in the pellet without polymerized MTs (data not shown).) The presence of RanGDP does not change the amount of MT-bound importin-β (81%). RanQ69L decreased importin-β binding to MTs resulting in 59% MT-bound importin-β. If both RanGDP and RanQ69L are present, the amount of MT bound importin-β (56%) is equal to that observed if RanQ69L is present alone which is in line with the observation that importin-β preferentially binds RanGTP. The experiments with recombinant wild-type importin-β reveal that importin-β can bind MTs directly, and the interaction decreases upon RanGTP binding. The binding of purified importin-β to MTs is much stronger than that observed in wild-type extract. It is most likely the consequence of the "naked" MTs compared to the extract where the MTs are highly decorated with MAPs; and also the extract certainly contains several soluble interacting partners for importin-β that affect the availability of importin-β for MTs. Of course, the results using the extract are expected to be closer to the in vivo conditions than results with purified importin-β. The RanGTP-insensitive pool (12%) observed in the wild-type extract may well be the result of the inherent ability of importin-β to bind MTs even in the presence of RanQ69L (Fig. 6B). The RanGTP-sensitive pool, on the other hand, can be due to the combination of both direct and MAP-mediated binding of MTs.

The binding of importin-β to certain types of MAPs either directly or through importin-α is not very surprising since several proteins including NuMA, TPX2, Eg5 have been shown to interact with importin-β (Gruss et al., 2001; Nachury et al., 2001; Wiese et al., 2001).

The observations summarized in Figures 4 and 5 suggest that P446L-imp-β binds stronger to MTs than normal importin-β. Indeed, both in the absence and in the presence of RanQ69L, more importin-β is bound to the MTs from the *Ketel*^{D}/+ extract than from the wild-type extract (Fig. 6A). Note that the *Ketel*^{D}/+extract contains wild-type importin-β and P446L-imp-β, thus the increased signal from the *Ketel*^{D}/+extract must come from the higher affinity of P446L-imp-β to MTs. Interestingly, the altered binding ability of P446L-imp-β is not merely due to not interacting with RanGTP and that way not releasing certain MAPs since the amount of MT-bound importin-β is higher in the *Ketel*^{D}/+extract than in the wild-type extract even in the cytoplasm-mimicking condition where Ran is in its GDP-bound form. If 50% wild-type importin-β content of the *Ketel*^{D}/+extract is assumed and that it has the same affinity toward MTs as observed in the wild-type extract, all the P446L-imp-β is likely to be bound to MTs under both conditions. The observations support the hypothesis that the increased MT-binding ability of P446L-imp-β counts for the *Ketel*^{D}-associated mutant phenotype, i.e. P446L-imp-β interferes with NE assembly by sequestering certain NE assembly factors onto the MTs.

Discussion

Importin-β was identified along elaborating the mechanism of nuclear protein import (Görlich and Kutay, 1999). During the past years the interacting partners – most importantly importin-α, Ran and some of the Nups – were identified and its molecular structure has been elucidated (Vetter et al., 1999; Cingolani et al., 1999; Lee et al., 2000). Along genetic dissection of the commencement of embryogenesis we identified the *Ketel* gene – by *Ketel*^{D} dominant female sterile mutations – that encodes the *Drosophila* homologue of importin-β (Lippai et al., 2000). The *Ketel*^{D} mutations block embryogenesis in dominant negative fashion, however not through the inhibition of nuclear protein import but by preventing NE reassembly at the end of cleavage mitosis suggesting involvement of importin-β in the process (Tirian et al., 2000). Analysis of the effects of P446L-imp-β, the *Ketel*^{D}-encoded protein, in injection experiments into *Drosophila* cleavage embryos confirmed the involvement of importin-β in NE assembly (Timinszky et al., 2002). Another characteristic feature of the *Ketel*^{D}mutations is an unusual formation of MT bundles and the persisting sperm aster MTs suggesting a relationship between importin-β and the MTs (Tirian et al., 2000). It has been confirmed in the meantime that importin-β is indeed a participant in mitotic spindle formation (Wiese et al., 2001; Nachury et al., 2001; Gruss et al., 2001) as well as in NE assembly (Timinszky et al., 2002; Zhang et al., 2002). In the present paper we describe the mode of action of P446L-imp-β by making use of an in vitro NE assembly system (Zhang and Clarke, 2000) to reveal novel features of importin-β in the processes and understand the basis of *Ketel*^{D}-related dominant female sterility.

As described in the Results section, *Drosophila* egg extracts support NE assembly over Ran- or importin-β-coated Sepharose beads as effectively as *Xenopus* egg extracts and thus make the bead system feasible to study NE assembly in vitro. Applicability of the bead system is also supported by the following observations. (*i*) The importin-β-coated beads initiate fast and efficient NE assembly around the beads and (*ii*) NE assembly does not take place over Ran-coated beads in *Xenopus* egg extracts from which importin-β had been depleted (Zhang et al., 2002).

Although functional NE assembly occurs in both the demembranated sperm chromatin and the Sepharose bead in vitro systems (Lohka and Masui, 1983; Zhang and Clarke, 2000), it is not clear whether the process proceeds through the same mechanism. In the chromatin system, NE assembly is believed to progress through the same steps as in vivo. The process of NE assembly is divided into distinct stages (Burke and Ellenberg, 2002; Hetzer et al., 2002). It begins during anaphase when the nucleus-derived vesicles bind to the chromosomes, fuse and flatten. Nucleoporins incorporate next in a stepwise fashion into the forming nuclear envelope until functional NPCs form. Nuclei form following the resumed import of nuclear proteins through the NPCs. It appears that components of the Ran system are involved in the membrane fusion event but not in vesicle targeting (Hetzer et al., 2001). The fact that Ran-coated beads attract vesicles raises the question as to what extent does the Ran-coated Sepharose system represent NE assembly in vivo. It was hypothesized recently that NE assembly proceeds in opposite fashion in the Ran-coated Sepharose system as over chromatin (Hetzer et al., 2002): NE vesicle targeting is based on interaction between importin-β and the Nups, that are embedded in the NE vesicles, and the subsequent fusion of the vesicles. Our in vivo results – based on injection of P446L-imp-β into wild-type cleavage embryos – support the model that NE assembly starts with importin-β-dependent vesicle targeting, since macromolecules persist in the chromatin area that would not be awaited if intact, continuous nuclear envelopes would form over the chromatin (Timinszky et al., 2002). Thus, an importin-β-mediated event preceding vesicle fusion occurs in NE assembly at least in the cleavage *Drosophila* embryos. The former proposition is supported by the finding that there is a high RanGTP concentration on chromatin (Kalab et al., 2002; Bilbao-Cortes et al., 2002) that is mimicked by Ran bound to the Sepharose beads in the in vitro bead system. It well may be that in a living cell both Ran-dependent and -independent vesicle targeting contribute to NE assembly, although in different cell types the contribution of the two mechanisms may be different.

Identical to the in vivo systems (Tirian et al., 2000; Timinszky et al., 2002), P446L-imp-β prevents NE assembly over the Ran-coated beads. The P446L-imp-β action is dominant negative since in *Drosophila* egg extracts containing normal importin-β besides P446L-imp-β (either prepared from *Ketel*^{D} eggs or from wild-type embryos into which P446L-imp-β had been added) NE formation is blocked. Apparently, the inhibitory effect of P446L-imp-β is only slightly reduced in eggs of females carrying one *Ketel*^{D} (P446L-imp-β coding) and up to as many as eight normal importin-β-encoding *Ketel* gene copies (our unpublished results). The inhibitory effect of P446L-imp-β is best explained by the binding of factors involved in targeting NE vesicles to chromatin that are available in limited amounts in the cytoplasm or in the egg extract. Possible targeting factors may be some of the Nups, many of which are known to interact with importin-β (Shah et al., 1998; Bayliss et al., 2000; Ben Efraim and Gerace, 2001), or a thus far unknown protein that functions as a link between NE vesicles and importin-β.

Unexpectedly, when bound to Sepharose beads P446L-imp-β induces NE assembly as efficiently as normal importin-β. It is rather unlikely that P446L-imp-β prevents NE assembly by dragging away the targeting factor(s) since Ran bound to Sepharose beads can itself interact with NE vesicles. As soon as NE vesicles are attracted over the beads by Ran or by wild-type importin-β, the vesicles can fuse in the vicinity of Ran (Hetzer et al., 2001) and the beads are covered by a continuous double membrane. However, if the targeting factors and/or the NE vesicles would be sequestered by P446L-imp-β and anchored in the cytoplasm (i.e. not available for NE assembly), the toxic effect of P446L-imp-β becomes understandable.

It appears that the structure to which P446L-imp-β is anchored are the MTs since a number of observations suggest that MTs are involved in regulation of importin-β function. (*i*) The nuclear import of parathormone-related protein was shown to be MT dependent (Lam et al., 2002). (*ii*) Most of the cytoplasmic importin-α coaligns with MTs and microfilaments in tobacco protoplasts (Smith and Raikhel, 1998). (*iii*) The KIF5B and KIF5C microtubular-based motor proteins bind to importin-β (Mavlyutov et al., 2002). (*iv*) Taxol has an inhibitory effect on nuclear protein import in digitonin-permeabilized HeLa cells (our unpublished data). (*v*) Under the rare experimental conditions when both intact nuclear envelopes and mitotic spindles are present at the same time (following the injection into cleavage *Drosophila* embryos of the p 25 protein, that disrupts MT function (Hlavanda et al., 2002)), nuclear protein import is inhibited (our unpublished data).

We set out to clarify features of importin-β-MT interaction hoping to understand the mode of dominant negative action of P446L-imp-β. Figure 6 presents evidence that importin-β binds MTs both directly and through MAPs. The effect of RanQ69L on MT-importin-β interaction shows that both types of binding are Ran sensitive. Assuming that RanQ69L abolishes cargo/MAP binding of importin-β, the 44% MT-bound importin-β in the wild-type extract in the absence of RanQ69L is mainly due to MAP-mediated binding. Whether the MT-importin-β binding has physiological significance or not remains to be elucidated. During interphase MTs may serve as routes directing importin-β with its cargo toward the nucleus. Experiments with the wild-type extract suggest that when Ran is loaded with GTP in the vicinity of chromatin, importin-β is released from the MTs (Fig. 6). During mitosis the MTs may function as depositories for factors involved in NE assembly that can be released upon disassembly of the mitotic spindle.

P446L-imp-β is strongly bound to MTs both in the absence and in the presence of RanGTP (Fig. 6A). The elevated MT-binding ability of P446L-imp-β is not merely due to its lost RanGTP-binding ability (Timinszky et al., 2002) and is likely to stem from both increased direct and indirect binding. (To our regret, instability of the purified P446L-imp-β under the experimental conditions did not allow us to gain more information on the mode of MT binding.) It appears thus that while P446L-imp-β attains increased MT-binding ability it binds nucleoporins as normal importin-β and prevents NE assembly through sequestering certain factors required for the process. However, it remains to be revealed what NE assembly factors are bound by P446L-imp-β.

Acknowledgements. We thank D. Görlich the generous supply of the "Ran mixture", I. Boros for providing the HeLa cells and J. Ovádi for tubulin and p 25. We are grateful for P. R. Clarke in whose lab the first pilot experiments were carried out. Support for the "Ketel project" came from several sources: OTKA T5537, OTKA 32540, AKP 96/2-590, ETT 660/96 to J. Szabad, an EMBO Short Term Fellowship (ASTF 9824) and a Békésy Fellowship to L. Tirián.

References

Bayliss, R., Littlewood, T., Stewart, M. (2000): Structural basis for the interaction between FxFG nucleoporin repeats and importin-beta in nuclear trafficking. Cell **102**, 99–108.

Ben Efraim, I., Gerace, L. (2001): Gradient of increasing affinity of importin beta for nucleoporins along the pathway of nuclear import. J. Cell Biol. **152**, 411–417.

Bilbao-Cortes, D., Hetzer, M., Langst, G., Becker, P. B., Mattaj, I. W. (2002): Ran binds to chromatin by two distinct mechanisms. Curr. Biol. **12**, 1151–1156.

Burke, B., Ellenberg, J. (2002): Remodelling the walls of the nucleus. Nat. Rev. Mol. Cell Biol. **3**, 487–497.

Cingolani, G., Petosa, C., Weis, K., Muller, C. W. (1999): Structure of importin-beta bound to the IBB domain of importin-alpha. Nature **399**, 221–229.

Cullen, C. F., Deak, P, Glover, D. M., Ohkura, H. (1999): mini spindles: A gene encoding a conserved microtubule-associated protein required for the integrity of the mitotic spindle in *Drosophila*. J. Cell Biol. **146**, 1005–1018.

Görlich, D., Kutay, U. (1999): Transport between the cell nucleus and the cytoplasm. Annu. Rev. Cell Dev. Biol. **15**, 607–660.

Gruss, O. J., Carazo-Salas, R. E., Schatz, C. A., Guarguaglini, G., Kast, J., Wilm, M., Le Bot, N., Vernos, I., Karsenti, E., Mattaj, I. W. (2001): Ran induces spindle assembly by reversing the inhibitory effect of importin alpha on TPX2 activity. Cell **104**, 83–93.

Hetzer, M., Gruss, O. J., Mattaj, I. W. (2002): The Ran GTPase as a marker of chromosome position in spindle formation and nuclear envelope assembly. Nat. Cell Biol. **4**, E177–E184.

Hetzer, M., Meyer, H. H., Walther, T. C., Bilbao-Cortes, D., Warren, G., Mattaj, I. W. (2001): Distinct AAA-ATPase p97 complexes function in discrete steps of nuclear assembly. Nat. Cell Biol. **3**, 1086–1091.

Hlavanda, E., Kovacs, J., Olah, J., Orosz, F., Medzihradszky, K. F., Ovadi, J. (2002): Brain-specific p25 protein binds to tubulin and microtubules and induces aberrant microtubule assemblies at substoichiometric concentrations. Biochemistry **41**, 8657–8664.

Kalab, P., Weis, K., Heald, R. (2002): Visualization of a Ran-GTP gradient in interphase and mitotic *Xenopus* egg extracts. Science **295**, 2452–2456.

Lam, M. H., Thomas, R. J., Loveland, K. L., Schilders, S., Gu, M., Martin, T. J., Gillespie, M. T., Jans, D. A. (2002): Nuclear transport of parathyroid hormone (PTH)-related protein is dependent on microtubules. Mol. Endocrinol. **16**, 390–401.

Lee, S. J., Imamoto, N., Sakai, H., Nakagawa, A., Kose, S., Koike, M., Yamamoto, M., Kumasaka, T., Yoneda, Y., Tsukihara, T. (2000): The adoption of a twisted structure of importin-beta is essential for the protein-protein interaction required for nuclear transport. J. Mol. Biol. **302**, 251–264.

Lippai, M., Tirian, L., Boros, I., Mihaly, J., Erdelyi, M., Belecz, I., Mathe, E., Posfai, J., Nagy, A., Udvardy, A., Paraskeva, E., Görlich, D., Szabad, J. (2000): The Ketel gene encodes a *Drosophila* homologue of importin-beta. Genetics **156**, 1889–1900.

Lohka, M. J., Masui, Y. (1983): Formation in vitro of sperm pronuclei and mitotic chromosomes induced by amphibian ooplasmic components. Science **220**, 719–721.

Mavlyutov, T. A., Cai, Y., Ferreira, P. A. (2002): Identification of RanBP2- and kinesin-mediated transport pathways with restricted neuronal and subcellular localization. Traffic **3**, 630–640.

Nachury, M. V., Maresca, T. J., Salmon, W. C., Waterman-Storer, C. M., Heald, R., Weis, K. (2001): Importin beta is a mitotic target of the small GTPase Ran in spindle assembly. Cell **104**, 95–106.

Shah, S., Tugendreich, S., Forbes, D. (1998): Major binding sites for the nuclear import receptor are the internal nucleoporin Nup153 and the adjacent nuclear filament protein Tpr. J. Cell Biol. **141**, 31–49.

Smith, H. M., Raikhel, N. V. (1998): Nuclear localization signal receptor importin alpha associates with the cytoskeleton. Plant Cell **10**, 1791–1799.

Timinszky, G., Tirian, L., Nagy, F. T., Toth, G., Perczel, A., Kiss-Laszlo, Z., Boros, I., Clarke, P. R., Szabad, J. (2002): The importin-beta P446L dominant-negative mutant protein loses RanGTP binding ability and blocks the formation of intact nuclear envelope. J. Cell Sci. **115**, 1675–1687.

Tirian, L., Puro, J., Erdelyi, M., Boros, I., Papp, B., Lippai, M., Szabad, J. (2000): The Ketel(D) dominant-negative mutations identify maternal function of the *Drosophila* importin-beta gene required for cleavage nuclei formation. Genetics **156**, 1901–1912.

Trieselmann, N., Wilde, A. (2002): Ran localizes around the microtubule spindle in vivo during mitosis in *Drosophila* embryos. Curr. Biol. **12**, 1124–1129.

Vetter, I. R., Arndt, A., Kutay, U., Görlich, D., Wittinghofer, A. (1999): Structural view of the Ran-importin beta interaction at 2.3 Å resolution. Cell **97**, 635–646.

Wiese, C., Wilde, A., Moore, M. S., Adam, S. A., Merdes, A., Zheng, Y. (2001): Role of importin-beta in coupling Ran to downstream targets in microtubule assembly. Science **291**, 653–656.

Zhang, C., Clarke, P. R. (2000): Chromatin-independent nuclear envelope assembly induced by Ran GTPase in *Xenopus* egg extracts. Science **288**, 1429–1432.

Zhang, C., Clarke, P. R. (2001): Roles of Ran-GTP and Ran-GDP in precursor vesicle recruitment and fusion during nuclear envelope assembly in a human cell-free system. Curr. Biol. **11**, 208–212.

Zhang, C., Hutchins, J. R., Muhlhausser, P., Kutay, U., Clarke, P. R. (2002): Role of importin-beta in the control of nuclear envelope assembly by Ran. Curr. Biol. **12**, 498–502.

TIMINSZKY GYULA–SZABAD JÁNOS

A sejtmaghártya élete

Kutatócsoportunk a *Ketel*^{D} ún. domináns nőstény-steril mutációkkal azonosította a muslica *Ketel*-génjét. A *Ketel*^{D}/+ nőstények petéi látszólag épek, meg is termékenyülnek, de bennük nem kezdődik el az embriógenezis. (A + jel az ép *Ketel*-gént szimbolizálja.) Azért nem, mert a sejtmagvak szétesnek, és miközben mikrotubuluskötegek képződnek, az embriók elpusztulnak. Következésképpen a *Ketel*^{D}/+ nőstények sterilek. Miután klónoztuk a *Ketel*-gént, kiderült, hogy az a muslica importin-β fehérjét kódolja. Meglepetésünkre azonban a *Ketel*^{D}-kódolt mutáns, az ún. P446L mutáns importin-β nem a sejtmagi fehérjeimportot gátolja, hanem a sejtmaghártya-képződést. A P446L importin-β az éptől mindössze egyetlen aminosavban különbözik: benne a 446. helyen nem prolin, hanem leucin van. Az importin-β és a P446L szerepét megértendő tekintettük át a sejtmaghártya életéről szóló ismereteket, és osztjuk meg az érdeklődő olvasókkal.

A magasabb rendű élőlények sejtjeinek egyik jellegzetessége a *sejtmag*. A sejtnek az az alkotója, amely a belsejében levő kromoszómákkal – pontosabban a kromoszómák DNS-ében kódolt genetikai információ alapján – meghatározza a sejtek felépítését és funkcióját. A sejtmagot a citoplazmától az a *sejtmaghártya* választja el, ami valójában két membrán sok-sok olyan „gyűrűvel" – *sejtmagpórus-komplexekkel* (angolul nuclear pore complex, NPC) –, amelyeken keresztül szabályozottan jutnak ki a molekulák a sejtmagból a citoplazmába, illetve a citoplazmából a sejtmagba. A sejtmaghártya külső rétege helyenként a citoplazmába türemkedik, ahol elágazik, ellapul, és az *endoplazmatikus retikulumot* (ER) képezi. A külső membrán lényegében az endoplazmatikus retikulum része. A belső membránhoz a heterokromatin egy része kapcsolódik, mintegy szilárd felszínt biztosítva a kromoszómák sejtmagon belüli elhelyezkedéséhez. A sejtmaghártya különlegessége, hogy a mitózis (sejtosztódás) kezdetén lebomlik, majd a végén újraalakul. Mi a sejtmaghártyának – mint szerkezeti elemnek – a szerepe? Hogyan szabályozott az anyagforgalom a sejtmagpóruskomplexeken át? Hogyan bomlik le, majd képződik újra a sejtmaghártya? Áttekintésünk az itt megfogalmazott kérdésekre ad választ.

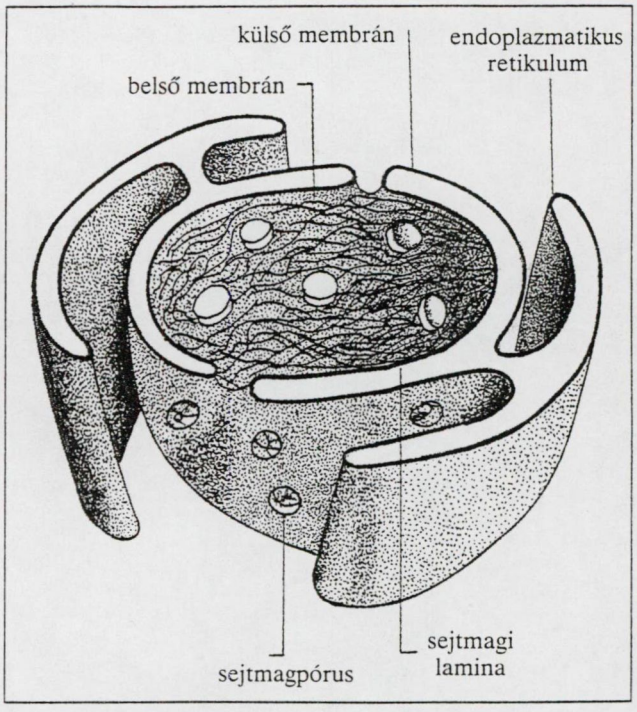

1. ábra. A sejtmag sematikus ábrázolása. A külső membrán a citoplazmába türemkedik, és az endoplazmatikus retikulumot képezi. A belső membrán felszínéhez a sejtmagbélés, az ún. sejtmagi lamina tapad. A lyukakba a sejtmagpóruskomplexek illeszkednek

A sejtmaghártya felépítése

A sejtmaghártya két membránból áll (**1. ábra**). A külső helyenként a citoplazmába türemkedik, ahol elágazik, ellapul, és az endoplazmatikus retikulumot képezi, nagy felületet biztosítva sok citoplazmatikus folyamathoz. A külső membrán a sejtmagpóruskomplexek szomszédságában áthajlik, és a belső membránban folytatódik. A külső és a belső membrán azért is különleges, mert bennük más-más fehérjék vannak. Amíg a külső membrán és az endoplazmatikus retikulum fehérjéi azonosak, addig a belső membrán sejtmagplazma felőli felszínéhez olyan speciális fehérjék tapadnak, amelyeknek négy típusát különböztetik meg. (i) A sejtmaghártya bélését – az ún. *sejtmagi laminát* – olyan rostos réteg alkotja, amely a laminafehérje-molekulák polimerizációja nyomán képződik *(1. és 2. ábra)*. A sejtmagi lamina biztosítja a sejtmaghártya és a sejtmagpóruskomplexek stabilizálását, és hozzá „kipányvázott" a kromoszómák heterokromatinjának legalább egy része, miközben az eukromatin – benne a génekkel – a sejtmag belsejébe nyúlik (**2. ábra**). (ii) A belső membrán alkotói azok a fehérjék, amelyekhez a sejtmagi lamina és heterokromatin is kapcsolódik. A belső membrán fehérjéi úgy képződnek az endoplazmatikus retikulumhoz tapadt riboszómákon, hogy közben az endoplazmatikus retikulum membránjába ékelődve maradnak. Később az endoplazmatikus retikulumban és a külső membránban diffundálva a belső membránba jutnak, ahol – mert kapcsolódnak az előbb említett sejtmagi fehérjékkel – megrekednek. (iii) A harmadik csoportba olyan kromatinfehérjék tartoznak, amelyek a sejtmagi laminával, illetve a belső membrán fehérjéivel teremtenek kapcsolatot. (iv) A negyedik csoportba a sejtmagpóruskomplexet alkotó ún. nukleoporin-fehérjéket sorolják. A sejtmagpóruskomplex a legnagyobb ismert fehérjekomplex: több mint húszféle fehérjéből épülnek fel, sejtmagpóruskomplexenként mindegyikből több kópiában. Egy sejtmaghártyán mintegy 2000-3000 sejtmagpóruskomplex van. Egy sejtmagpóruskomplex lényegé-

ben egy 120 nm széles és 40 nm vastag fehérjegyűrű, amely átível a sejtmaghártya mindkét membránján (**3. ábra**). Egy-egy sejtmagpóruskomplex sugaras szimmetriába szerveződött nyolc fehérjekomplexet alkot. A henger belsejében 40 nm átmérőjű csatorna van. Egy-egy NPC-ből nyolc nukleoporinfehérje fonálként nyúlik a citoplazmába, és mintegy antennaként gyűjtik össze azokat a molekulákat, amelyek útja előbb az NPC-khez, majd a sejtmagba vezet. Egy-egy NPC-ből kiindulva nyolc, gyűrűvel összekötött nukleoporin-fonál – „kosárka" – illeszkedik a sejtmagplazmába. A kosárkák azok a helyek, ahol a sejtmagba importált komplexek szét-, a sejtmagból exportálódó komplexek pedig összeszerelődnek. Lényegében tehát a sejtmagpóruskomplexek biztosítják az összes szabályozott anyagforgalmat a sejtmag és a citoplazma között. Úgy tűnik, hogy a nukleoporinoknak nem csak a sejtmagpóruskomplexeken át történő szállításban van szerepük. Mind a sejtmagi laminával, mind a kromatinnal kapcsolódnak, és szabályozzák azok szerkezetét, funkcióját.

Élet a sejtmaghártyán

A sejtmaghártya élete szorosan kapcsolódik a sejt életciklusához. A sejt életében két fő szakaszt szokás elkülöníteni: az egyiket *interfázis*nak, a másikat *mitózis*nak nevezik. Az interfázisban a sejtek a rájuk jellemző funkciókat látják el, és növekszenek. A mitózis során a sejtek legömbölyödnek, majd kettéosztódnak. A mitózis végén két leánysejt képződik, amelyek interfázisba kerülnek. Az interfázisok és a mitózisok végtelen körforgásként követik egymást, és alkotják a sejtciklusokat. Az interfázis folyamán két fontos esemény történik: a DNS replikációja, valamint különféle típusú fehérjemolekulák szintézise. Minthogy fehérjemolekulák csak a citoplazmában képződnek, a replikációban szorgoskodó fehérjék, valamint a kromatinfehérjéknek ugyanúgy importálódniuk kell a sejtmagba, mint azoknak a fehérjéknek, amelyek a sejtmag szerkezeti elemei, vagy azoknak, amelyek szabályozzák a gének kifejeződését. Ugyanakkor a sejtmagból a citoplazmába kell exportálódniuk azoknak az mRNS-eknek, amelyek alapján a fehérjemolekulák képződnek és azoknak a riboszómáknak is, amelyek a sejtmagvacskában képződnek, és a fehérjeszintézis aktív szereplői. A sejtmag és a citoplazma közötti anyagforgalom a sejtmagpóruskomplexeken keresztül történik. Hogyan?

A sejtmagi transzportfolyamatok mechanizmusa

A sejtmagpórusok csatornája 40 nm „széles", és rajta csak a nagyon kicsi molekulák diffundálhatnak át szabadon. A nagyobb molekulákat a sejtmagpóruskomplexeken csatornába türemkedő fehérjéi strázsaként feltartóztatják. A fehérjemolekulák közül csak azok juthatnak a sejtmagba, amelyeknek része egy speciális jel, az ún. *sejtmagi lokalizációs szignál* (angolul nuclear localization signal, NLS). A sejtmagi lokalizációs szignál a sejtmagba importálandó fehérjemolekulák jellegzetes, 7-10 aminosavból álló szakasza, amelyek között gyakori a pozitív töltésű *lizin* és az *arginin*. A sejtmagi lokalizációs szignálhoz a citoplazmában az *importin-β* fehérje kapcsolódik vagy közvetlenül, vagy egy adaptermolekulán keresztül, és ez viszi a sejtmagpóruskomplexek citoplazmatikus felszínéhez, ahol az ún. *importkomplexek dokkolnak* (**4. és 5. ábra**). Miközben az importkomplexet az NPC-k belsejét bélelő nukleoporionk „kézről kézre adják", beviszik a sejtmaghártya belső oldalán levő kosárkába. A sejtmag belsejében a RanGTP várja az importkomplexet, és miközben kivonja az importin-β-t a komplexből, szabaddá válik a sejtmagi fehérje *(4. ábra)*. A RanGTP–importin-β komplex a sejtmagpóruskomplexeken keresztül exportálódik a sejtmagból a citoplaz-

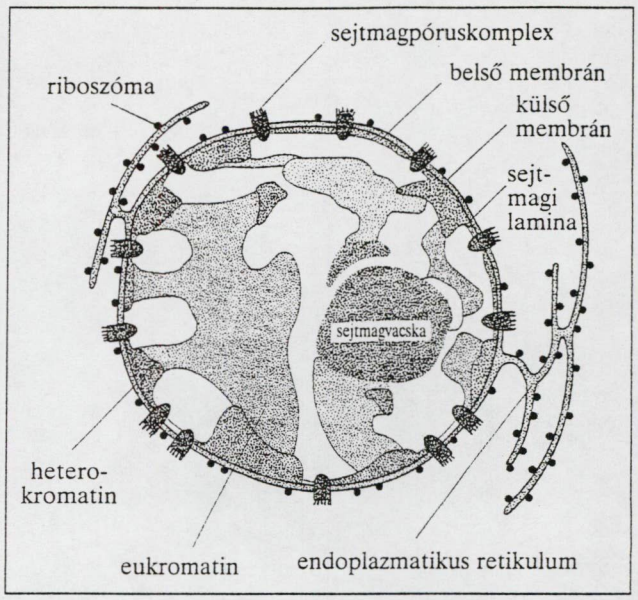

2. ábra. A sejtmag keresztmetszete bemutatja a belső alkotókat és azok elhelyezkedését

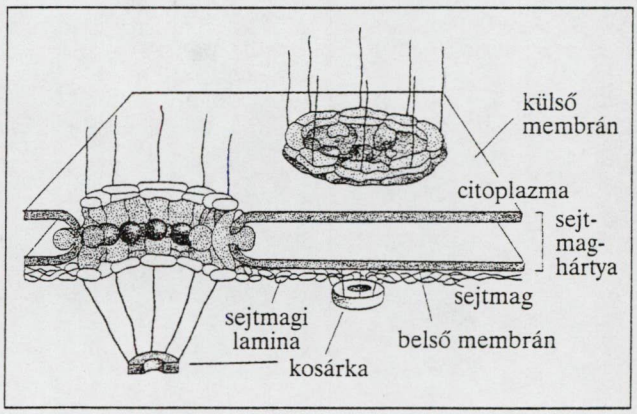

3. ábra. A sejtmagpóruskomplex felépítése

4. ábra. A sejtmagi fehérjeimport (bal oldalon) és az mRNS-export (jobb oldalon) mechanizmusának sematikus ábrázolása

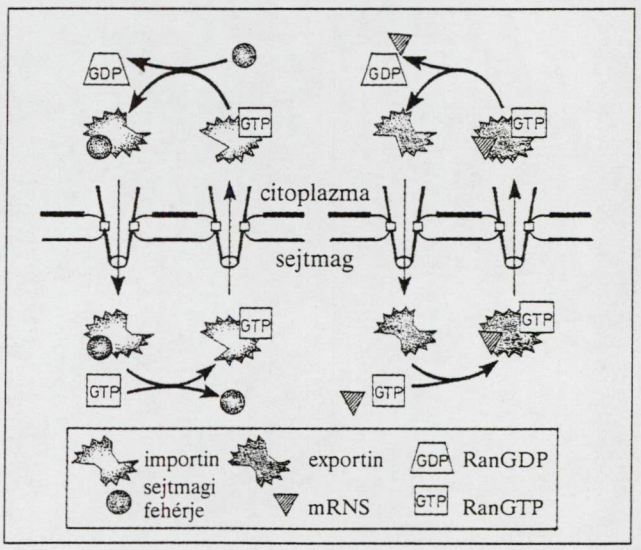

mába, ahol miközben a RanGTP RanGDP-vé alakul, az importin-β szabaddá válik, hogy újabb importciklust kezdjen. A RanGDP a sejtmagba importálódik, ahol RanGTP-vé alakul, és várja a következő importkomplexet. A folyamat mozgatója az a Ran fehérje, amely a sejtmagban GTP-, a citoplazmában GDP-kötött formában van. A sejtmagi fehérjeimporthoz szükséges energia pedig a GTP › GDP hidrolízisből ered.

Az mRNS-ek és például a riboszómák útja az ellenkező irányba vezet: a sejtmagból a citoplazmába. A sejtmagi exportfolyamatnak az az *exportin* a legfontosabb részvevője, amely az importinok rokona, és amely funkcióját a Ran fehérje szabályozza: az exportin akkor szállít ki valamit a sejtmagból, ha Ran is kapcsolódik hozzá, és akkor tér vissza a sejtmagba, ha Ran nem kötődik hozzá (*4. ábra*).

A sejtmaghártya és a kromatin kapcsolata

A sejtmaghártya belső rétege és a hozzá kapcsolódó bélés – a sejtmagi lamina – egyrészt stabilizáló szerkezeti elem, másrészt olyan felszín, amelyhez például a kromoszómák bizonyos részei kapcsolódnak, lehetőséget biztosítva a génműködés szabályozásához. (Sejtmagi lamina hiányában a sejtmagpóruskomplexek a sejthártyában nem szétszórtan, hanem összecsapzódva helyezkednek el, ami miatt a sejtek életképtelenek.) Nagy általánosságban igaz az a megállapítás, hogy minél fejlettebb egy élőlény, annál többféle sejt- és szövettípus alkotja, és annál többféle olyan fehérjefélesége van, amely a sejtmaghártya belső felszínével kapcsolódik. Jó megközelítéssel igaz az az összefüggés, hogy minél magasabb rendű egy élőlény, annál nagyobb a genomjának mérete, annál több génje van, és annál bonyolultabb génműködésének szabályozási mechanizmusa. A kromoszómák sejtmagon belüli elrendeződéséhez, a génkifejeződés szabályozásához a sejtmaghártya belső felszíne biztosít alapot. (A feladat nem csekély, hiszen az interfázisú, mintegy 5 µm átmérőjű emberi sejtmagban csaknem kétméternyi DNS van úgy becsomagolva negyvenhat kromoszómába, hogy a kromatin – a kromoszómák anyaga – a sejtmag térfogatának csak mindössze 5%-át teszi ki.) Interfázisban a kromoszómák laza szerkezetűek, hogy a gének kifejeződhessenek. A mitózis kezdetére viszont feltekeredned (szupertekercselődnek), és azt a közismert tömör formát veszik fel, amelyben a mitózis során az utódsejtek között megoszlanak.

A kromoszómáknak két jellegzetes része van. Az egyik a centromer szomszédságában levő *heterokromatin*, amely géneket vagy nem, vagy csak néhányat tartalmaz, és kromatinja mindig, a mitózis során pedig különösen erősen feltekeredett. A másik az *eukromatin*, ami a kromoszómáknak az a része, amely a géneket tartalmazza. Azon részei lazák, ahol az aktív gének vannak, lehetővé téve a gének kifejeződését. Az eukromatin olyan részei viszont tömörek, ahol az inaktív, nem működő gének vannak. A kromatin tömör részei – a heterokromatin és az eukromatin inaktív része – a sejtmaghártya belső felszínéhez vannak kikötve. (Éppen úgy, mint a Barr-test, ami nem más, mint a nőkben az inaktiválódott egyik X-kromoszóma anyaga.) Megfigyelték, hogy amíg a kromatinnak az aktív géneket tartalmazó részei a sejtmag belsejében vannak, ugyanakkor azokban a sejttípusokban, amelyekben ugyanazok a gének inaktívak, a kromatin a sejtmaghártya belső membránjához tapad. Azt is leírták, hogy a legtöbb olyan, a génműködést szabályozó fehérje, amely géneket kapcsol be vagy ki, a belső membránhoz kötődik. Érthető tehát, hogy a belső membrán fehérjeösszetételének változása nyomán megváltozik a belső membránhoz kapcsolódó kromatin mennyisége, és vele együtt bizonyos gének szabályozásának mechanizmusa is. A legújabb eredmények alapján úgy tűnik, hogy vannak olyan daganattípusok, amelyek az itt említett ok miatt alakulnak ki. Az is tudott, hogy a *lamin*-, valamint az *emerin*génekben bekövetkező mutációk úgy változtatják meg a sejtmaghártya belső membránjának fehérjeösszetételét, szerkezetét, hogy az a rendellenes génkifejeződés nyomán szívizom-elváltozásokhoz, szívnagyobbodáshoz vezet.

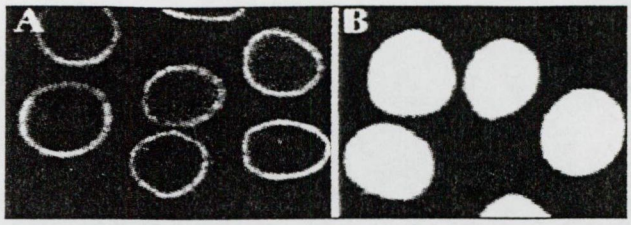

5. ábra. (A) A fluoreszcensen jelölt sejtmagi fehérje kapcsolódik az importin-β-val, és – a sejtmagpóluskomplexeken átjutáshoz szükséges energia hiányában – az importkomplexek dokkolnak a sejtmagpóruskomplexek citoplazmatikus felszínén. (B) Energiaforrás jelenlétében a sejtmagi fehérje a sejtmagba importálódik, és azt „kivilágítja" (Az ábra konfokális mikroszkópban készült optikai metszeteket mutat)

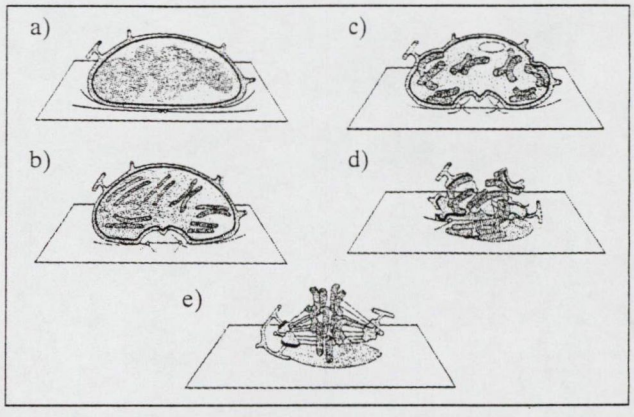

6. ábra. A sejtmaghártya szétszerelődésének sematikus ábrázolása. Az interfázist (a) követően a kromoszómák kondenzálódnak, a centroszómák eltávolodnak egymástól (b). A mikrotubulushoz kapcsolódó motormolekulák feszítik a sejtmaghártyát, amely a centroszómákkal átellenben szétszakad (c). A sejtmaghártya-maradványt a motormolekulák lefejtik a kromoszómákról, és a centroszómákhoz szállítják (d). A sejtmaghártya membránja a mitózis alatt az endoplazmatikus retikulum részévé válik, a centroszómák pedig megszervezik az osztódási orsót (e)

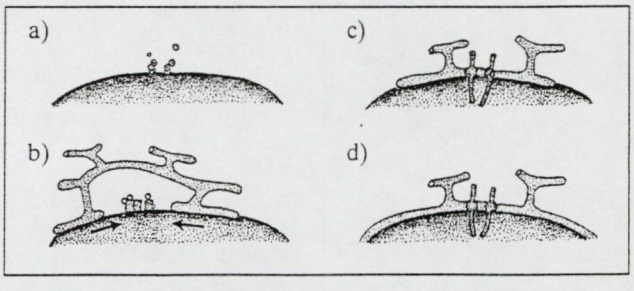

7. ábra. A sejtmaghártya összeszerelődésének mechanizmusa. Először a sejtmagpóruskomplex fehérjéi kapcsolódnak a kromatinhoz (a). A sejtmagpóruskomplexek kialakulása közben a sejtmaghártyát alkotó membrán darabkái is kapcsolatot teremtenek a kromatinnal (b). A sejtmagpórusok beágyazódnak a sejtmaghártyába (c). A sejtmaghártya membrándarabkái fuzionálnak, kialakítva az összefüggő sejtmaghártyát (d)

A sejtmaghártya szét- és összeszerelődése

A sejtosztódás a sejtek életének egyik legfontosabb és talán legkritikusabb szakasza. Csak akkor kezdődhet el, amikor a DNS már replikálódott, a kromatin pedig úgy tömörödött kromoszómákká, hogy „kényelmesen", részek elvesztése nélkül lehet őket a képződő két leánysejtbe juttatni. Ahhoz, hogy a kromatin tömörödhessen, szabaddá kell válnia, le kell válnia a sejtmaghártya belső felszínéről. A megoldás a következő: a mitózis kezdetén – a ciklin-ciklin függő kinázkomplex tevékenysége nyomán – a sejtosztódásban szerepet játszó fehérjék nagy része foszforilálódik, köztük a sejtmagi lamina és a belső membrán fehérjéinek némelyike. A foszforiláció nyomán a fehérjék térszerkezete és aktivitása is megváltozik, a fehérjék közötti kölcsönhatások megszűnnek, és végeredményben a sejtmaghártya szétszerelődik (**6. ábra**). Alkotóinak némelyike az endoplazmatikus retikulum részévé válik, mások a citoplazmában oldott állapotban vannak. A sejtmaghártya szétszerelődése nyomán nyílik lehetőség a kromatin tömörödésére, a kromoszómák képződésére.

A sejtmaghártya lebomlásának nem a foszforiláció az egyetlen mozgatórugója. A sejtmaghártyát alkotó molekulákat azok az ún. motormolekulák fejtik le a kromoszómákról, amelyek a mikrotubulus-nyalábokhoz kapcsolódnak, és miközben a mikrotubulusok mentén vándorolnak, a sejtmaghártya komponenseit az endoplazmatikus retikulumba szállítják. A mikrotubulusok a sejtváz csodálatra méltó „szerkezetei": az interfázisra jellemző pályaszerkezetük előbb lebomlik, majd mire a kromoszómák kialakulnak, mitotikus orsóvá szerveződnek, hogy pályaként szolgáljanak a kromoszómák szétválásának. Az említett motormolekulák most a kromoszómákat szállítják a sejt két ellentétes pólusához.

A mitózis végén a sejtmaghártyának újra ki kell alakulnia. A sejtmaghártya összeszerelődésének első lépéseként a sejtmagpórusokat felépítő fehérjék némelyike a kromoszómákhoz kapcsolódik (**7. ábra**). A foszfolipidmembrán komponensei csak a következő lépésben kapcsolódnak a kromatinhoz. Kezdetben minden egyes kromoszómát sejtmaghártya burkol be. Az összefüggő sejtmaghártya kialakulásában olyan fehérjék működnek közre, melyek a foszfolipidmembránok fúzióját végzik, sőt – bár szerepe még nem ismert pontosan – a sejtmaghártya kialakulásához a sejtmagi transzportfolyamatoknál megismert Ran is szükséges. A minden egyes kromoszómát magába foglaló, jellegzetes interfázisú sejtmaghártya kialakulásához minden bizonnyal szükség van olyan fehérjékre is, amelyeket ma még nem ismerünk, a lekerekedett sejtmag pedig azután alakul ki, miután újraindulnak a sejtmagi importfolyamatok.

Amíg a sejtciklus interfázisában mikrotubulusok csak a citoplazmában vannak, a kromoszómák a sejtmagba vannak zárva. Ahhoz, hogy osztódási orsók képződjenek, a mikrotubulusoknak és a kromoszómáknak egy térrészbe kell kerülniük. Két lehetőség képzelhető el. (1) Az egyik, hogy az ún. zárt mitózis során a mikrobutulusok jutnak be a sejtmagba és képeznek osztódási orsót (mint pl. az élesztősejtekben). (2) A másik, hogy a nyílt mitózis során a sejtmaghártya felbomlik, miáltal a mikrotubulusok kapcsolatba kerülhetnek a kromoszómákkal (mint pl. az emberi sejtekben). Sőt egyes fajokban a zárt és nyitott mitózis közti átmenet is megfigyelhető. Úgy tűnik, hogy amíg a bonyolult felépítésű sejtmaghártya megkívánja a teljesen nyitott mitózist, az egyszerűbb felépítésű sejtmaghártya esetében a mitózis lehet zárt, vagy félig nyitott. Meglehet, hogy a szabályozásbeli előnnyel járó összetettebb sejtmaghártya vonzata az a látszólag értelmetlen folyamat, hogy tudniillik a mitózis kezdetén a sejtmaghártya szét-, a végén pedig összeszerelődik. Egy biztos: bár a sejtmaghártya életének néhány mozzanatát már ismerjük, még mindig sok titkot rejteget.

Csavarvonalak

Az ammonitesz spirálja

Felsőörsről származó ammonitesz *(Kellneritesfelsoeoersensis; Vörös Attila gyűjtése)*

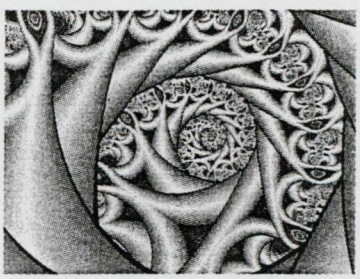

Fraktális kanyarok *(Robert Carr munkája)*

A természet és az emberi kéz gyakran hoz létre spirális formát. A DNS „kettős csavar"-járól és más makromolekulákról – melyek szerkezetét sokszor szemléltetik csigavonalban futó szalagokkal – a 146. és a 154. oldalon olvashatnak. Címképünk csigalépcsője régi mesterek műve. Egyik illusztrációnkon számítógéppel készített fraktálkép ismétli meg a csavarvonalat. Alábbi írásunk kővé vált, spirális puhatestűekről szól.

Az ammoniteszek igen gyakori ősmaradványai azoknak az üledékes kőzeteknek, amelyek a paleozoikum (földtörténeti ókor) közepe és a mezozoikum (földtörténeti középkor) vége között, egykori tengerekben lerakódott üledékekből képződtek. A ma élő Nautilus távoli rokonsági körébe tartozó ammoniteszek a puhatestűek, azon belül a lábasfejűek egyik kihalt csoportját alkotják. Kamrákra tagolt, a nemzetségek többségének esetében síkban felcsavarodott külső mészvázukat bordák és csomók díszítik. Erre a jellegzetes spirális formára utal az „ammonitesz" elnevezés is, amely a kosszarvú egyiptomi isten, Ámon nevéből ered.

Az ammoniteszek a mezozoikum legjobb „vezérkövületei". Változatos megjelenésüknek, rövid fajöltőjüknek, valamint tengeri úszólebegő életmódjukból fakadó nagy földrajzi elterjedésüknek köszönhetően kiválóan alkalmasak arra, hogy segítségükkel a geológusok a különböző korú rétegekből felépülő rétegsorokat az ősmaradvány-tartalmuk alapján tagolják, illetve, hogy egymástól távoli területek rétegsorait egymással párhuzamosítsák.

Az ammoniteszek mintegy 380 millió évvel ezelőtt jelentek meg, és a kréta végén, mintegy 65 millió évvel ezelőtt haltak ki. Törzsfejlődésük korántsem nevezhető folyamatos „sikertörténetnek". A paleozoikum során fellépő viszonylag kis számú nemzetségüket a perm és a triász fordulóján lezajlott kihalás alaposan megtizedelte. Virágkorukat a mezozoikum során élték, de a triász és a jura határán kis híján kipusztultak. Ezt a krízist túlélve érték el pályafutásuk „csúcsát" a jura során, a kréta végi kihalást azonban már az ammoniteszek sem vészelték át.

Hol találkozhatunk Magyarországon ezeknek a kihalt élőlényeknek a kövületeivel? Középhegységeink triász, jura és kréta korú tengeri üledékes képződményeiben keresgélhetünk eséllyel ammoniteszek után, ezek közül is elsősorban a Bakony és a Gerecse, valamint a Mecsek és a Villány mészkő- és márgarétegeiben. Több fajukat és nemzetségüket hazánk területén írták le először, ami sokszor nevükben is kifejeződik (Balatonites, Arpadites, Hungarites stb.). Gyönyörű metszeteik figyelhetők meg egyes épületek burkolatán is, például néhány budapesti metróállomás vörös mészkő lapokkal fedett padlóján.

BUDAI TAMÁS